AIMS Mathematics, 11(5): 14025–17074.
DOI: 10.3934/math.2026577
Received: 11 February 2026
Revised: 23 April 2026
Accepted: 07 May 2026
Published: 18 May 2026

https://www.aimspress.com/journal/Math

Research article

Applications of the novel extended Rayleigh distribution in statistical quality, censored data with application for engineering materials

Laila A. Al-Essa[1], **Muhammad Imran**[2] **and Farrukh Jamal**[3,*]

[1] Department of Mathematical Sciences, College of Science, Princess Nourah bint Abdulrahman University, Riyadh, Saudi Arabia; Laalessa@pnu.edu.sa

[2] Assistant Director (Statistics), Agriculture Department, Government of Punjab, Pakistan; imranshakoor84@yahoo.com

[3] Department of Statistics, Faculty of Science, University of Tabuk, Tabuk, Saudi Arabia

* **Correspondence:** Email: fshakir@ut.edu.sa; Tel: +966511740230.

Abstract: We introduce an extended three-parameter Rayleigh distribution using the genesis of a truncated discrete Bell distribution. The expressions for the rth moment, Réyni entropy, and quantile function are presented. Moreover, a group acceptance sampling plan for a truncated life test using the median as a quality parameter is presented. Two estimation methods (classical and Bayesian) are used to estimate parameters. The practical relevance of the proposed model is demonstrated using two real-life datasets related to engineering materials. Bias and efficiency of the estimators are assessed through simulation. Additionally, we present a censored data application using data centered on the survival rates of kidney patients ($n = 76$, censored = 23.7%, event = 76.3%). However, the Kaplan–Meier survival curve supports the proposed exponentiated Bell Rayleigh distribution.

Keywords: acceptance sampling; Bayes estimation; Bell distribution; censored data; maximum likelihood estimation; statistical quality control
Mathematics Subject Classification: 60E05, 62E15, 62F15, 62N01, 62P30

1. Introduction

Classical distributions such as normal, exponential, and gamma are commonly implemented and offered robust foundations for statistical inference; however, the increasing heterogeneity and complexity of empirical data have highlighted their limitations. In fact, these distributions are based on limited assumptions such as symmetry, light tails, or fixed hazard functions. To overcome these challenges, a key solution is the development of generalized probability distributions, which offer greater flexibility and accuracy in handling complex data patterns [1]. Lord Rayleigh (1880)

developed the Rayleigh distribution (RD) [2], which has extensive applications in acoustics, wind speed modeling, reliability engineering, survival analysis, and signal processing. Basically, it is a simple special case of the Weibull distribution with a shape parameter equal to two. The cumulative distribution function (CDF) of the RD is as follows:

$$H(t) = 1 - \exp\left(-\frac{t^2}{2\alpha^2}\right), \qquad t > 0, \tag{1.1}$$

where $\alpha > 0$ is the only scale parameter. However, Eq (1.1) has a simple closed-form solution, but it has some practical issues. They are as follows: (i) It is incapable of modeling nonmonotonic hazard rates or decreasing hazard rates, which are common in biomedical, survival analysis, and engineering reliability data; (ii) It cannot control skewness or tail thickness because its shape parameter is limited to two (limiting shape flexibility); (iii) Heavy and light tails cannot be modeled; and (iv) It is unable to model multimodal lifetime data. Due to these complexities, several extended versions of RD have been presented by incorporating extra parameters and functional transformations with improved goodness of fit measures. Here, we go through some useful extensions of the RD, such as that from Kundu and Raqab [3], which is useful to address the nonmonotonic failure rates. Cordeiro et al. [4] proposed the flexible four-parameter extended RD with multiple failure rate patterns, including nonmonotonic hazard rates, using the beta-G family of distributions. Moreover, Cordeiro et al. [5, 6] proposed useful extensions of the RD that include applications in regression analysis. Al-Babtain introduced a type-I half-logistic RD [7]. Merovci extended the RD using the record-based transmuted-G family [8]. Another useful three-parameter extension of the RD using the Weibull-X family given by [9]. MirMostafaee et al. [10] proposed an RD extension using Marshall–Olkin settings. Similarly, Jose and Sivadas proposed another useful extension of the RD by compounding it with a truncated negative binomial [11]. Bantan et al. presented the unit-RD for bounded intervals [12]. Gómez et al. [13] proposed another extension of RD by compounding the Rayleigh and Lindley discrete distributions.

In contemporary quality assurance systems (aerospace, pharmaceuticals, and other high-reliability sectors), acceptance sampling plans are essential, especially in regulated industries, manufacturing, and logistics. Conversely, there are many situations where 100% inspection of the products is impractical due to high costs, time constraints, or the destructive nature of tests. Thus, without performing an intensive inspection, these acceptance sampling plans offer a statistically reliable framework for deciding to accept or reject a lot under inspection. These sampling plans are simple to implement and improve operational efficiency and lower costs. These plans act as a safety net between suppliers and customers, balancing the risks of the manufacturer (the likelihood of rejecting a good lot) and the consumer (the likelihood of accepting a bad lot) within defined limits. A group acceptance sampling plan (GASP) offers several advantages, including a smaller sample size requirement than single and double acceptance sampling plans, economical destructive life tests, increased reliability assurance, and quicker decision-making (due to the plan's ability to test several items at once) [14–16]. Numerous studies are presented to design a GASP using advanced probability models which are based on truncated lifetime; we mention a few. See, for example, Nwankwo et al. [17], Hafeez et al. [18], Fayomi and Khan [19], Imran et al. [20], Algarni [21], and Almarashi et al. [22]. Despite, the Bayesian estimation's complexity, modern statistical computing tools make it possible. Numerous studies offer conceptual frameworks to estimate parameters of the extended

models using Bayesian estimation (BE). They are as follows: Okasha et al. [23] used the Marshall–Olkin extended inverse Weibull distribution; Afify et al. [24] employed a new inverse Weibull distribution; Aslam et al. [25] proposed an economic design of a group acceptance sampling plan under the Bayesian frameworks; El-Morshedy et al. [26] applied the exponentiated generalized inverse flexible Weibull distribution; and Eldessouky et al. [27] applied a Bayesian method to a new extension of the Kumaraswamy exponential.

This study addresses three main aspects. In the first part, we present the exponentiated Bell Rayleigh (EBR) distribution in connection with the truncated Bell distribution; for more detail, readers are referred to [28, 29]. Moreover, we construct a GASP for a truncated life test using the median as a quality parameter [22]. We present the two estimation methods, including maximum likelihood estimation (MLE) and BE, and the design parameters are obtained under both estimation methods. Two real data applications are presented, including the breaking stress of carbon fibers [22] and the Kevlar 373/epoxy time to failure [19]. In the second part of the study, we present a censored data application of the proposed EBR distribution using kidney patient survival data. The Kaplan–Meier (KM) survival curves are also obtained for the EBR distribution, exponentiated RD and, RD under both estimation methods. Below are some compelling reasons and benefits of using the EBR distribution:

- The proposed EBR distribution shares many characteristics with the Bell distribution and can handle overdispersion as well as heavy-tailed data.
- Its nonmonotonic hazard rate function, along with other useful shapes, makes it an intriguing tool for reliability, survival, and quality control analysis.
- It is ideal for highly skewed data.
- It is ideal for quantile regression analysis, actuarial analysis, and acceptance sampling due to its closed-form quantile function.
- It is useful for censored data analysis because of its simple CDF.

The paper is organized as follows: In Section 2, the construction and some basic properties of the EBR distribution are presented. Section 3 focuses on the construction of a GASP when an item's lifetime follows the EBR distribution. Section 4 illustrates the two estimation methods, MLE and BE. Simulation studies under both estimation methods are presented in Section 5. Two real-data applications are demonstrated in Section 6. In Section 7, the censored data application is presented. Finally, Section 8 is devoted to concluding remarks with future recommendations.

2. The proposed exponentiated Bell RD

System reliability is quantified using statistical models based on probability theory and stochastic processes. Many industrial components experience material deterioration and operational damage. These processes occur gradually over time under normal working conditions. As a result, the performance of the system decreases, and the system may eventually fail. Thus, statistical models play a crucial role in predicting and monitoring reliability for industrial and engineering systems and ensuring system safety [30–32]. Consider a system consisting of R independent subsystems all working at a given specific time, and assume that all are independent and identically distributed (IID). Suppose that t_1 is the life of the first subsystem, t_2 is the life of the second subsystem, and so on, and t_i

is the life of the ith subsystem. Each subsystem further consists of parallel β components. A series system will completely fail if any one of its components fails. On the other side, if any subsystem fails in parallel structures, the entire system fails. For better understanding here, we consider a system based on subsystem components C_1–C_3. Components C_1–C_3 are connected in a parallel system so that the subsystem still works if either C_1, C_2, or C_3 works (as shown in Figure 1). On the other side, components C_1 and C_2 are connected in a series system (as shown in Figure 2); that subsystem only works if both components C_1 and C_2 work [33].

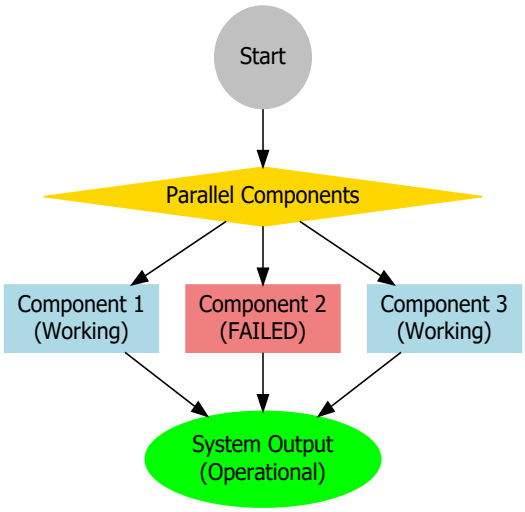

Figure 1. A graphic illustration of a parallel system.

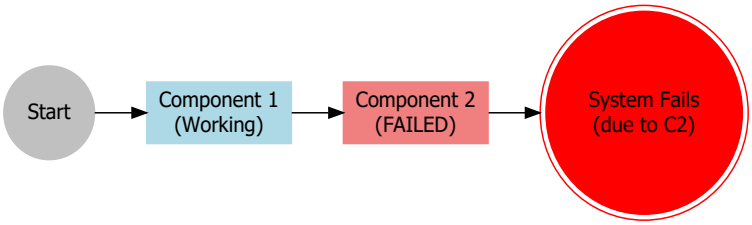

Figure 2. A graphic illustration of a series system.

2.1. Construction

Let us assume a system having R subsystems connected in a series configuration. Let R be a positive real-valued random variable that follows a zero-truncated Bell distribution with PMF:

$$P(R = r) = \frac{\lambda^r \exp\left(1 - e^{\lambda}\right) \Xi_r}{r! \left[1 - \exp\left(1 - e^{\lambda}\right)\right]}, \quad r \geq 1, \tag{2.1}$$

where $\lambda > 0$ and Ξ_r are the Bell numbers. The lifetime of the ith subsystem is denoted by T_i, and each subsystem consists of β parallel units with $C_{i,1}, \ldots, C_{i,\beta}$, where $C_{i,1}$ denotes the first unit inside the tth subsystem. Assume that units inside subsystems follow Eq (1.1). Following [34], if Z =

$\min(T_1, T_2, \cdots, T_R)$, then the unconditional CDF of Z is given by

$$W_Z(t) = 1 - \left(\frac{\exp\left(1 - e^{\lambda}\right)}{1 - \exp\left(1 - e^{\lambda}\right)} \right) \sum_{r=1}^{\infty} \frac{\left[\lambda \left(1 - \left[1 - \exp\left(-\frac{t^2}{2\alpha^2} \right) \right]^{\beta} \right) \right]^r}{r!} \Xi_r. \tag{2.2}$$

Using Bell numbers' well-known relationship [29], it is as follows:

$$\exp\left(e^t - 1\right) = \sum_{r=0}^{\infty} \frac{t^r}{r!} \Xi_r. \tag{2.3}$$

After comparing Eq (2.2) with Eq (2.3), the CDF of the EBR distribution is obtained as follows:

$$W(t) = \frac{1 - \exp\left\{ -e^{\lambda} \left[1 - \exp\left(-\lambda \left\{ 1 - \exp\left(-\frac{t^2}{2\alpha^2} \right) \right\}^{\beta} \right) \right] \right\}}{1 - \exp\left(1 - e^{\lambda}\right)}, \quad t > 0. \tag{2.4}$$

For Eq (2.4), the PDF is as follows:

$$w(t) = \lambda\beta \frac{t}{\alpha^2} \exp\left(\frac{-t^2}{2\alpha^2} \right) \left[1 - \exp\left(-\frac{t^2}{2\alpha^2} \right) \right]^{\beta-1} \exp\left(\lambda - \lambda \left[1 - \exp\left(-\frac{t^2}{2\alpha^2} \right) \right]^{\beta} \right) \tag{2.5}$$
$$\exp\left\{ -e^{\lambda} \left[1 - \exp\left(-\lambda \left\{ 1 - \exp\left(-\frac{t^2}{2\alpha^2} \right) \right\}^{\beta} \right) \right] \right\} \left[1 - \exp\left(1 - e^{\lambda}\right) \right]^{-1},$$

where $\alpha > 0$, $\beta > 0$, and $\lambda > 0$. If $\beta = 1$, it reduces to a Bell RD. The parameters: α governs the scale of failure times, β controls the shape of the hazard behavior, and λ affects the distribution's tail behavior and flexibility. Figure 3 presents the PDF shapes at varying parametric values of α, λ, and β, which indicates low β, a sudden early peak; high β, a somewhat right peak– but still heavy in the early stages for small $\alpha = 1.5$ and large $\lambda = 4.2$ (a high prevalence of early failures and short lifespans). Similarly, low β indicates an earlier peak; high β, heavier tails and a tilt to the right for $\alpha = 1.8$ and $\lambda = 1.5$ (equal likelihood of failures in early and midlife). For small λ, it yields a flattened start with low β and a lengthy right tail with a delayed peak with high β (a low prevalence of early failures and long lifetime behavior). Numerous social and scientific investigations frequently encounter these phenomena, demonstrating the practical relevance of the proposed distribution.

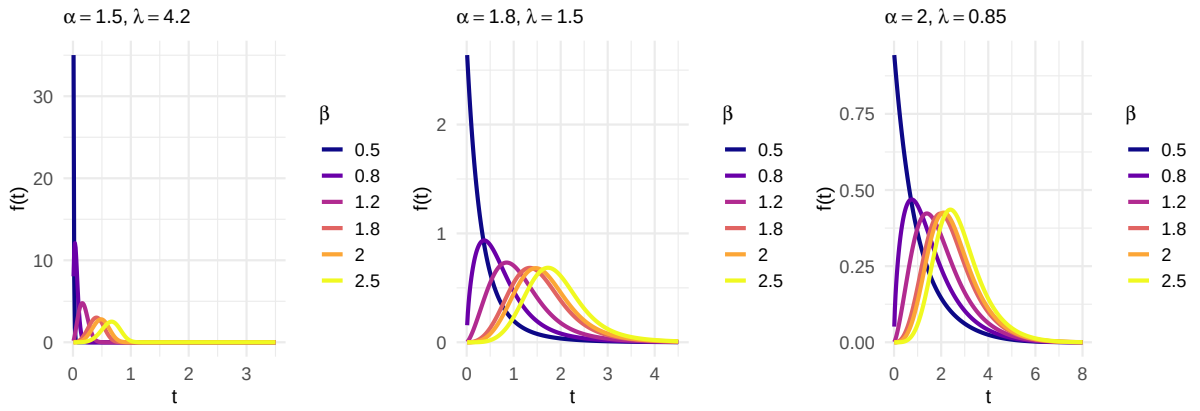

Figure 3. PDF plotting at different parametric values.

Conversely, Figure 4 illustrates the shapes of failure rates. It includes increasing, increasing-decreasing, and bathtub shapes (high rates at the beginning, low in the middle, and high again at the end). These hazard rate shapes provide insights into how the likelihood of failure changes over time, which is crucial for predicting product lifespan and maintenance needs. The hazard rate classifications are as follows:

$$\begin{cases} \beta > \frac{1}{2} \Rightarrow \text{increasing–decreasing (unimodal)}, \\ \beta = \frac{1}{2} \Rightarrow \text{approximately constant initially}, \\ \beta < \frac{1}{2} \Rightarrow \text{decreasing hazard rate}. \end{cases} \tag{2.6}$$

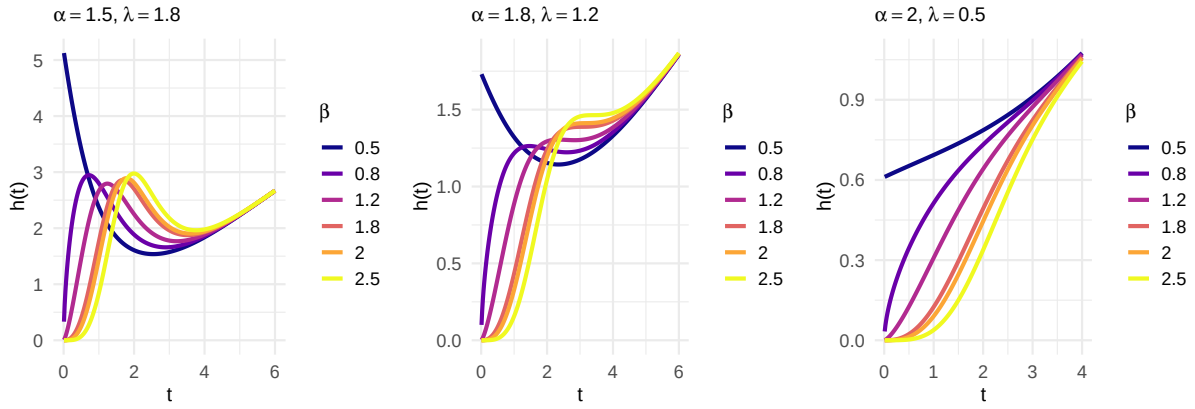

Figure 4. Hazard rate function plotting at different parametric values.

2.2. *Identifiability conditions and limiting behavior*

Identifiability is the state in which various parameter values produce different probability distributions. For Eq (2.4), the identifiability conditions are:

- $\alpha > 0$: To guarantee a valid time/space domain, the scale parameter must be strictly positive.
- $\beta > 0$: To keep the CDF monotonic, the shape parameter must be strictly positive.
- To prevent a degenerate distribution in which the denominator or internal exponents become constant, the parameter λ needs to be nonzero.

Mathematically, if

$$W(t;\lambda_1,\alpha_1,\beta_1) = W(t;\lambda_2,\alpha_2,\beta_2) \Rightarrow (\lambda_1,\alpha_1,\beta_1) = (\lambda_2,\alpha_2,\beta_2), \tag{2.7}$$

for all t, then $(\lambda_1,\alpha_1,\beta_1)$ must equal to $(\lambda_2,\alpha_2,\beta_2)$. Because the parameters (λ,α,β) are uniquely determined by the equality of the CDF for all $t > 0$, the proposed distribution is identifiable. Moreover, the proposed distribution is a valid CDF because its limiting behavior satisfies $\lim_{t\to 0^+} W(t) = 0$ and $\lim_{t\to\infty} W(t) = 1$.

2.3. *Log-concavity*

The distribution's shape and whether it is unimodal with a distinct peak can be ascertained using log-PDF convexity (or concavity). Additionally, it is crucial because it ensures that maximum likelihood estimators in statistical inference are stable and unique.

Theorem 2.1. *When $\beta > 0.25$, the EBR density in Eq* (2.5) *is log-concave.*

Proof.

$$\ell(t) = \log w(t) = \log t + \frac{t^2}{2\alpha^2} + (\beta - 1)\log\left(1 - \exp\left[-t^2/(2\alpha^2)\right]\right) \\ + \log\left(1 - \exp\left[-\lambda H(t)\right]\right) - \exp(\lambda)\left(1 - \exp\left[-\lambda H(t)\right]\right), \tag{2.8}$$

where

$$H(t) = \left(1 - \exp\left[-t^2/(2\alpha^2)\right]\right)^{\beta}.$$

The first differentiate $\ell'(t)$ with respect to t is given by

$$\ell'(t) = \frac{1}{t} + \frac{t}{\alpha^2} + (\beta - 1)\frac{g(t)}{G(t)} + \lambda H'(t)\exp\left[-\lambda H(t)\right]\left(\frac{1}{(1 - \exp\left[-\lambda H(t)\right])} - \exp(\lambda)\right), \tag{2.9}$$

where

$$G(t) = 1 - \exp\left[-t^2/(2\alpha^2)\right], \quad g(t) = \frac{t}{\alpha^2}\exp\left(\frac{t^2}{2\alpha^2}\right) \quad \text{and} \quad H'(t) = \beta G(t)^{\beta-1} g(t).$$

To get the initial convexity requirement, we focus on the behavior as $t \to 0$: $G(t) \sim t^2/2\alpha^2$; $g(t) \sim t/\alpha^2$; $g(t)/G(t) \sim 2/t$. The term $\exp\left[-\lambda H(t)\right] = 1$ as $t \to 0$, and

$$1 - \exp\left[-\lambda H(t)\right] \sim 1 - \left[1 - \lambda H(t)\right] = \lambda H(t)$$

using the Taylor expansion. After simplification and substitution, Eq (2.8) becomes

$$\ell'(t) = \frac{1}{t} + (\beta - 1)\frac{g(t)}{G(t)} + \beta\frac{g(t)}{G(t)^{\beta}}, \tag{2.10}$$

$$\ell'(t) = \frac{1}{t} + (\beta - 1)\frac{2}{t} + \beta\frac{2}{t} = \frac{4\beta - 1}{t}. \tag{2.11}$$

The second derivate is given by

$$\ell''(t) = -\frac{4\beta - 1}{t^2}. \tag{2.12}$$

The log-density is concave when

$$\beta > 0.25 \Rightarrow \ell''(t) < 0,$$

indicating a well-behaved and stable shape. It is convex when $\beta < 0.25$. □

Figures 5 and 6 show the graphical analysis of the convexity analysis of log-density for two cases: when $\beta > 0.25$ and when $\beta < 0.25$.

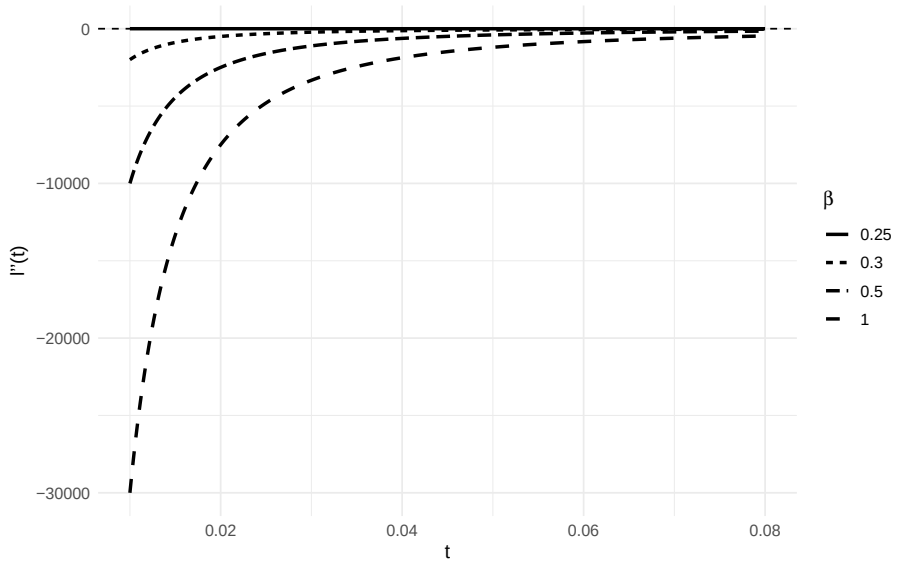

Figure 5. A graphic demonstration of the convexity analysis of log-density when $\beta > 0.25$.

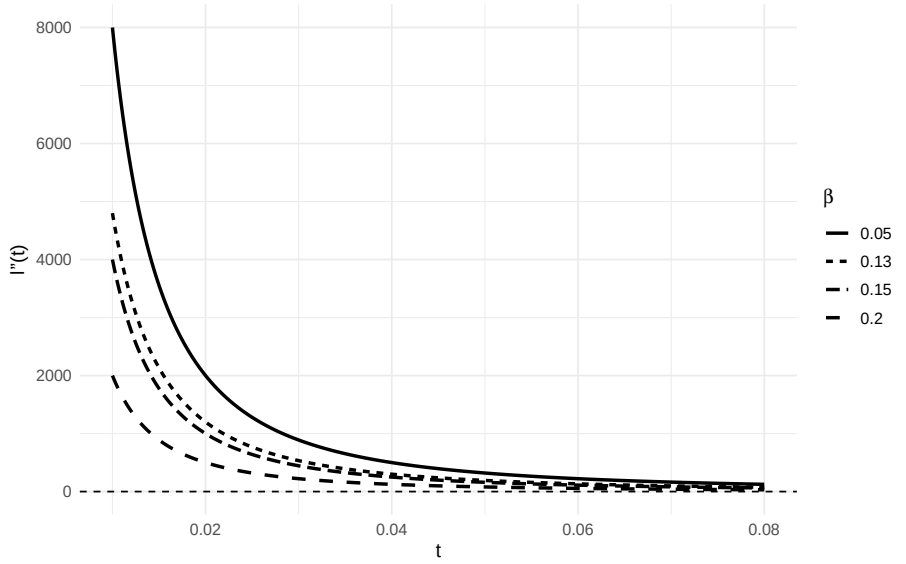

Figure 6. A graphic demonstration of the convexity analysis of log-density when $\beta < 0.25$.

2.4. Asymptotic behavior

The proposed model exhibits flexible behavior at the origin, depending on the shape parameter β, whereas the tail is dominated by an exponentially decaying Rayleigh-type structure. Therefore, the model ensures light-tailed behavior and suitability for lifetime data modeling. The asymptotic behavior of the proposed model is given by

$$w(t) \sim \begin{cases} C_1\, t^{2\beta-1}, & t \to 0, \\ C_2\, t \exp\left(-\frac{t^2}{2\alpha^2}\right), & t \to \infty, \end{cases} \tag{2.13}$$

where C_1 and C_2 are positive constants.

2.5. *Quantile function*

The quantile function (QF) of the EBR distribution is derived by inverting Eq (2.4) with respect to t. It is given by

$$t_p = \alpha \sqrt{-2 \ln\left(1 - \{-\lambda^{-1} \ln\left[1 + e^{-\lambda} \ln\left(1 - p\left[1 - \exp\left(1 - e^{\lambda}\right)\right]\right)\right]\}^{\frac{1}{\beta}}\right)}, \tag{2.14}$$

where $p \in (0, 1)$ follows the uniform distribution. The QF holds a closed-form representation, thereby facilitating its uses in practical applications such as acceptance sampling plans, quantile regression, and the derivation of L-moments. However, the median of the distribution is obtained by setting $p = 0.5$ in Eq (2.14).

Figure 7 shows a visual summary of the QF at different parametric settings. Quantiles with higher λ increase more slowly and smoothly, whereas those with a smaller λ expand more quickly at lower p but reach saturation faster. For small p, the $\beta < 1$ curve climbs quickly, and for the $\beta > 1$ curve, accelerates later (longer lower tail). This demonstrates the QF's adaptability in many applied domains for delicate systems where early-life failures predominate. It is appropriate for balanced systems where the risk of failure is distributed more evenly across time. For instance, in consumer electronics, this could be used to calculate maintenance intervals or replacement cycles. It can be used for high-reliability systems (such as aircraft parts, electronic devices, and medicine), where quantiles are used to simulate service life in mission planning and specify extended inspection intervals.

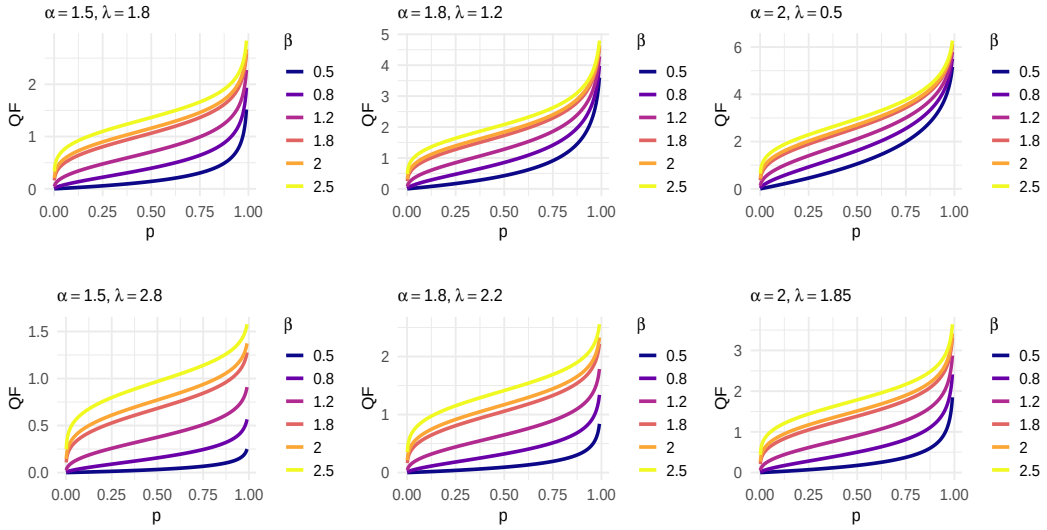

Figure 7. QF plotting at different parametric values.

2.6. *rth moment*

Proposition 2.1. *The rth moment of the EBR distribution is given by*

$$\mu'_r = \sum_{\Upsilon=0}^{\infty} \mathcal{H}_{\Upsilon} \frac{2^{\frac{r}{2}}\, \alpha^r}{(1 + \Upsilon)^{\frac{r}{2}+1}} \Gamma\left(\frac{r}{2} + 1\right), \tag{2.15}$$

where

$$\mathcal{H}_{\Upsilon} = \frac{\lambda^{1+g}\beta}{[1-\exp(1-e^{\lambda})]g!}\sum_{p=0}^{\infty}\sum_{m,g=0}^{\infty}\frac{1}{p!}(-1)^{p+m+g+\Upsilon}\binom{\beta(g+1)-1}{\Upsilon}\binom{p}{m}(1+m)^{g}e^{\lambda(1+p)}.$$

Proof. Here, we use the two main generic formulas: the binomial expansion and the power series for exponential functions. They are as follows, respectively:

$$(1-\omega)^{s} = \sum_{k=0}^{\infty}(-1)^{k}\binom{s}{k}\omega^{k}, \qquad |\omega| < 1, \tag{2.16}$$

where $\binom{s}{k}$ denotes the generalized binomial coefficient, and

$$\exp(-wt^{c}) = \sum_{p=0}^{\infty}(-1)^{p}\frac{(wt^{c})^{p}}{p!}, \tag{2.17}$$

for any real numbers w, c and t. Equation (2.5) can be expressed as follows:

$$w(t) = \frac{\lambda\beta g(t)G(t)^{\beta-1}e^{\lambda}e^{-\lambda G(t)^{\beta}}\exp\left(-e^{\lambda}\left[1-e^{-\lambda G(t)^{\beta}}\right]\right)}{1-\exp(1-e^{\lambda})}, \tag{2.18}$$

where

$$G(t) = 1-\exp\left(-\frac{t^{2}}{2\alpha^{2}}\right) \quad \text{and} \quad g(t) = \frac{t}{\alpha^{2}}\exp\left(\frac{-t^{2}}{2\alpha^{2}}\right).$$

By using Eq (2.17) to the last term of Eq (2.18), we get

$$\exp\left(-e^{\lambda}\left[1-e^{-\lambda G(t)^{\beta}}\right]\right) = \sum_{p=0}^{\infty}(-1)^{p}e^{p\lambda}\left(1-e^{-\lambda G(t)^{\beta}}\right)^{p}. \tag{2.19}$$

The final power term can be constrained as follows using Eq (2.16):

$$\left(1-e^{-\lambda G(t)^{\beta}}\right)^{p} = \sum_{m=0}(-1)^{m}\binom{p}{m}e^{-\lambda m G(t)^{\beta}}. \tag{2.20}$$

After simplification, Eq (2.18) reduces as given by

$$w(t) = \frac{\lambda\beta g(t)G(t)^{\beta-1}}{1-\exp(1-e^{\lambda})}\sum_{p=0}^{\infty}\sum_{m=0}(-1)^{p+m}\binom{p}{m}\frac{e^{\lambda(1+p)}}{p!}e^{-\lambda G(t)^{\beta}(1+m)}. \tag{2.21}$$

Using exponential series to the last term of Eq (2.21), we obtain

$$e^{-\lambda G(t)^{\beta}(1+m)} = \sum_{g=0}^{\infty}(-1)^{g}\frac{[\lambda(1+m)]^{g}}{g!}G(t)^{g\beta}. \tag{2.22}$$

By substituting Eq (2.22) in Eq (2.21), we obtain

$$w(t) = \frac{\lambda}{[1-\exp(1-e^{\lambda})]}\sum_{p=0}^{\infty}\sum_{m,g=0}^{\infty}(-1)^{p+m+g}\binom{p}{m}\frac{e^{\lambda(1+p)}(1+m)^{g}\lambda^{g}}{p!g!}\beta g(t)G(t)^{\beta(g+1)-1}. \tag{2.23}$$

Consider the last term in Eq (2.23),

$$I = g(t)G(t)^{\beta(g+1)-1}dt.$$

It is as follows:

$$I = g(t)G(t)^{\beta(g+1)-1} = \frac{t}{\alpha^2}\exp\left(\frac{-t^2}{2\alpha^2}\right)\left[1-\exp\left(-\frac{t^2}{2\alpha^2}\right)\right]^{\beta(g+1)-1}. \tag{2.24}$$

By applying Eq (2.16), the above expression is further simplified as follows:

$$I = g(t)G(t)^{\beta(g+1)-1} = \sum_{\Upsilon=0}^{\infty}(-1)^{\Upsilon}\binom{\beta(g+1)-1}{\Upsilon}\frac{t}{\alpha^2}\exp\left[\frac{-t^2}{2\alpha^2}(1+\Upsilon)\right]. \tag{2.25}$$

By replacing Eq (2.25) in Eq (2.23), we solve

$$\mu'_r = \int_0^{\infty}\frac{t^{r+1}}{\alpha^2}\exp\left[\frac{-t^2}{2\alpha^2}(1+\Upsilon)\right]dt,$$

which completes the proof of Proposition 2.1. □

Equation (2.15) can be used to obtain the mean and variance of the EBR distribution, taking $r = 1$ and

$$\sigma^2 = \mu'_2 - (\mu'_1)^2.$$

The Pearson coefficients of skewness (γ_1) and kurtosis (γ_2), respectively, can be computed as

$$\gamma_1 = \sqrt{\mu_3^2/\mu_2^3}$$

and

$$\gamma_2 = \left(\mu_4/\mu_2^2\right) - 3.$$

The well-known functional relationship between ordinary and mean moments can be used to derive the mean moments using Eq (2.15). The mean and variance increase as β increases, but skewness and kurtosis decrease, indicating a shift from unpredictable early failures to more consistent reliability. However, a small β results in short-lived, highly skewed, and heavy-tailed lifespan distributions, which are useful to model fragile components or systems that have an early-failure mode. Conversely, a higher β yields a more systematic and lighter-tailed distribution, which is suitable for systems with stable and predictable lifetimes. When λ is small, the variance tends to decrease (as shown in Figure 9). Table A.1 presents a numerical overview of μ, σ^2, γ_1, and γ_2 at some parametric values (see Appendix). A graphic overview of μ, σ^2, γ_1, and γ_2 is presented in Figures 8 and 9.

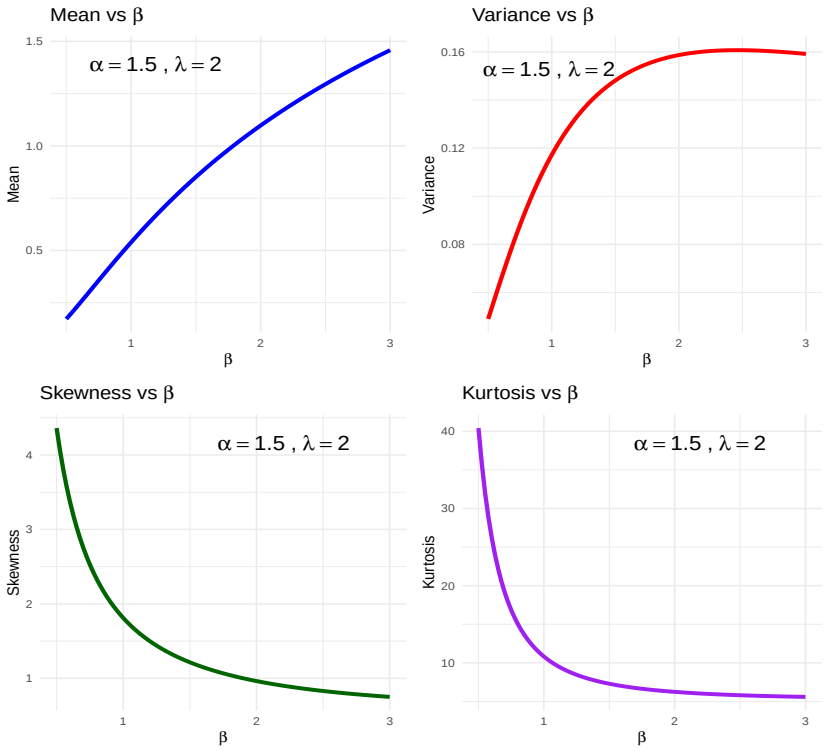

Figure 8. A graphic representation of μ, σ^2, *skew*, and *kurt* in relation to β.

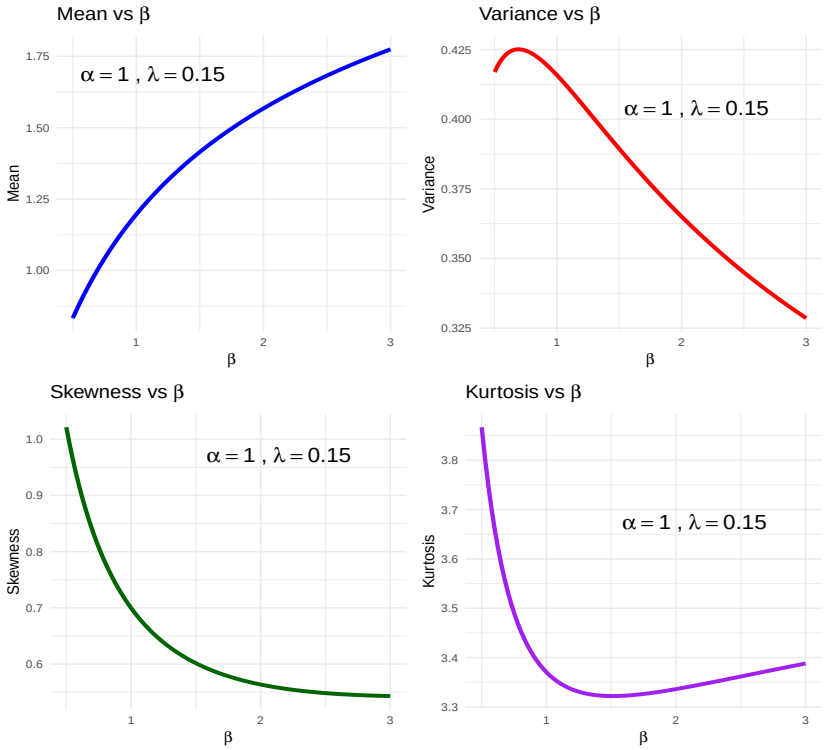

Figure 9. A graphic demonstration of μ, σ^2, γ_1, and γ_2 in relation to β.

2.7. *Réyni entropy*

Réyni entropy (RE) is a general measure of uncertainty in a probability distribution. It is frequently used to examine distributional uncertainty in information theory and reliability research. It is defined as

$$\mathbb{H}_a(T) = \frac{1}{1-a}\log\left(\int w(t)^a\, dt\right),$$

where $a > 0$, and $a \neq 1$. Let T be a random variable with a PDF defined in Eq (2.5). Then, the RE of order a for $a > 0$ and $a \neq 1$, corresponding to the EBR distribution, is given by

$$\mathbb{H}_a(T) = (1-a)^{-1}\log\left(\sum_{\xi=0}^{\infty}\hbar_\xi \frac{2^{\frac{a-1}{2}}\,\alpha^{1-a}\,\Gamma\left(\frac{a+1}{2}\right)}{(a+\xi)^{\frac{a+1}{2}}}\right), \tag{2.26}$$

where

$$\hbar_\xi = \frac{\beta^a\lambda^{(a+z)}e^{a\lambda}}{z!\left[1-\exp\left(1-e^{\lambda}\right)\right]^a}\sum_{z=0}^{\infty}\sum_{u=0}^{\infty}\sum_{n=0}^{\infty}\frac{1}{u!}(-1)^{u+n+z+\xi}\binom{\beta z + a(\beta-1)}{\xi}\times\binom{u}{n}\left(ae^{\lambda}\right)^u(n+a)^z. \tag{2.27}$$

The RE is lowest when β and λ are large with a large (strong peak focus), and maximum when β and λ are small (weak peak), as given in Table A.2. A positive value indicates higher uncertainty or more randomness in the distribution, whereas a negative value indicates very low uncertainty. Moreover, a graphic demonstration (as shown in Figures 10–12) also supports the numerical findings (see Table A.2 in the Appendix). This suggests that the proposed EBR distribution exhibits notable flexibility, capturing a wide range of distributional shapes, from highly dispersed to sharply peaked, through variation in β, λ, and a. The model's uncertainty is extremely sensitive to the shape parameter β, as shown in Figures 10–12. The observed decrease in entropy with increasing β implies that a considerable reduction in distributional spread is possible when the Rayleigh baseline is compounded with the Bell distribution. In high-precision engineering, where failure times are strictly limited within a predicted window, this feature is especially advantageous.

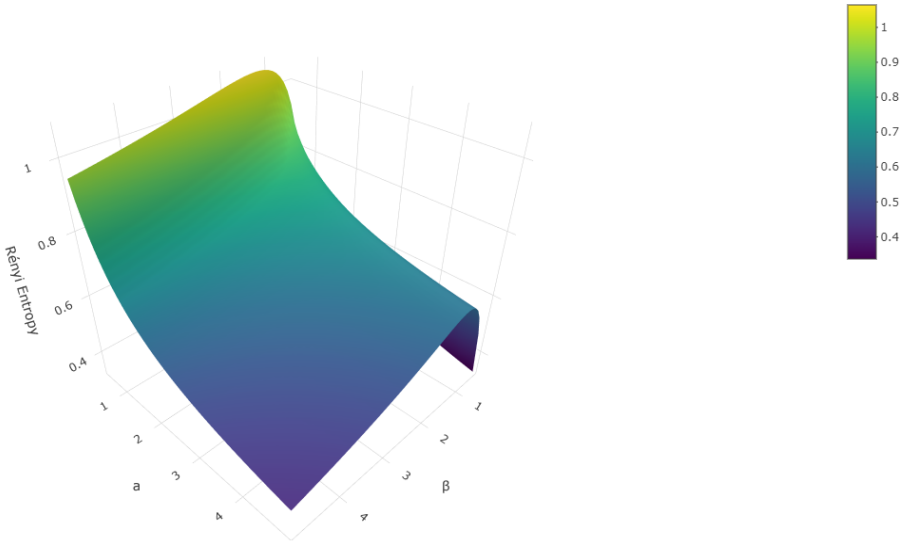

Figure 10. A graphic representation of the RE for $\alpha = 1$, $\lambda = 0.3$.

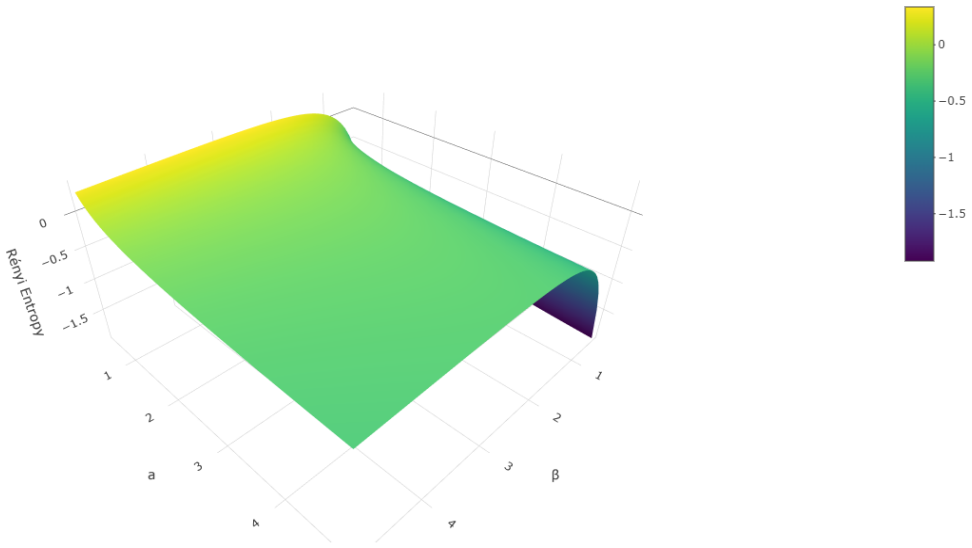

Figure 11. A graphic representation of the RE for $\alpha = 1$, $\lambda = 2$.

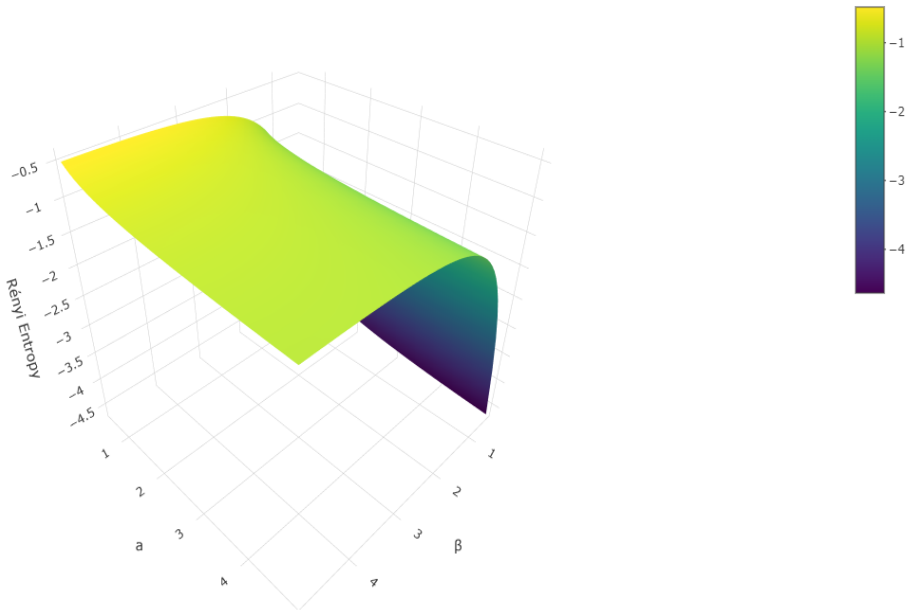

Figure 12. A graphic representation of the RE for $\alpha = 1$, $\lambda = 4$.

2.8. Stochastic ordering

Stochastic ordering provides a reliable method for comparing random variables, making choices, and comprehending risk or reliability. It is used in reliability engineering for comparing component lifetimes. In finance and insurance, we can choose the best financial or insurance policy or investment without knowing the precise distributions. It allows us to understand how the distribution in survival or

regression models is impacted by parameter changes. Suppose that we have two random variables T_1 and T_2. Assume $T_1 \sim F_1(t)$ with survival function $\bar{F}_1(t) = 1 - F_1(t)$ and PDF $f_1(t)$. Similarly, assume $T_2 \sim F_2(t)$ with survival function $\bar{F}_2(t) = 1 - F_2(t)$ and PDF $f_2(t)$. For a specific arrangement, the random variable T_1 is regarded as stochastically smaller than T_2:

- Stochastic order: $T_1 \leq_{st} T_2 \iff \bar{F}_1(t) \leq \bar{F}_2(t), \quad \forall t$;
- Likelihood ratio order: $T_1 \leq_{lr} T_2 \iff f_1(t)/f_2(t)$ is decreasing in $t \geq 0$;
- Hazard rate order: $T_1 \leq_{hr} T_2 \iff \bar{F}_1(t)/\bar{F}_2(t)$ is decreasing in $t \geq 0$;
- Reversed hazard rate order: $T_1 \leq_{rhr} T_2 \iff F_1(t)/F_2(t)$ is decreasing in $t \geq 0$.

Above, all four of the stochastic orders are related to one another, with the following implications [35, 36]:

$$T_1 \leq_{\text{rhr}} T_2 \impliedby T_1 \leq_{lr} T_2 \implies T_1 \leq_{\text{hr}} T_2 \implies T_1 \leq_{st} T_2.$$

Theorem 2.2. *Assume $T_1 \sim EBR(\lambda_1, \alpha, \beta)$ and $T_2 \sim EBR(\lambda_2, \alpha, \beta)$. If $\lambda_1 < \lambda_2$, then $T_1 \leq_{lr} T_2$.*

Proof. First, we have the log ratio using Eq (2.5):

$$\begin{aligned} \log\left[\frac{w_1(t)}{w_2(t)}\right] = \log\left(\frac{\lambda_1}{\lambda_2}\right) + (\lambda_1 - \lambda_2) + \log\left(\frac{C_2}{C_1}\right) \\ + (\lambda_2 - \lambda_1)H(t) + e^{\lambda_2\left[1-e^{-\lambda_2 H(t)}\right]} - e^{\lambda_1\left[1-e^{-\lambda_1 H(t)}\right]}, \end{aligned} \tag{2.28}$$

where

$$H(t) = \left(1 - e^{-t^2/(2\alpha^2)}\right)^{\beta}, \quad C_i = 1 - \exp\left(1 - e^{\lambda_i}\right), \ i = 1, 2.$$

If $\lambda_1 < \lambda_2$, we obtain

$$\frac{d}{dt}\log\left[\frac{w_1(t)}{w_2(t)}\right] = \frac{\beta x}{\alpha^2}\left[1 - e^{-t^2/(2\alpha^2)}\right]^{\beta-1} e^{-t^2/(2\alpha^2)}\left[(\lambda_2 - \lambda_1) + \lambda_2 e^{\lambda_2[1-H(t)]} - \lambda_1 e^{\lambda_1[1-H(t)]}\right] < 0, \tag{2.29}$$

where

$$H(t) = \left(1 - e^{-t^2/(2\alpha^2)}\right)^{\beta}.$$

Because

$$\frac{d}{dt}\log\frac{w_1(t)}{w_2(t)} \leq 0,$$

for all $t > 0$, it follows that $w_1(t)/w_2(t)$ is decreasing in t. Hence,

$$T_1 \leq_{lr} T_2.$$

This completes the proof. □

3. A group acceptance sampling plan

To determine the optimization of a GASP, the two design parameters, such as c, the acceptance number, and g, the total number of groups, are very important. The cost and duration of inspections in an experiment depend on these two design parameters. An inappropriate design parameters' selection

results in erroneous conclusions, either accepting a poor lot or rejecting a good lot. The aim of this section is to optimize the design parameters for the truncated life test. The following steps, as shown in Figure 13, can be taken to determine the design parameters when the product's or item's lifetime aligns with the EBR distribution:

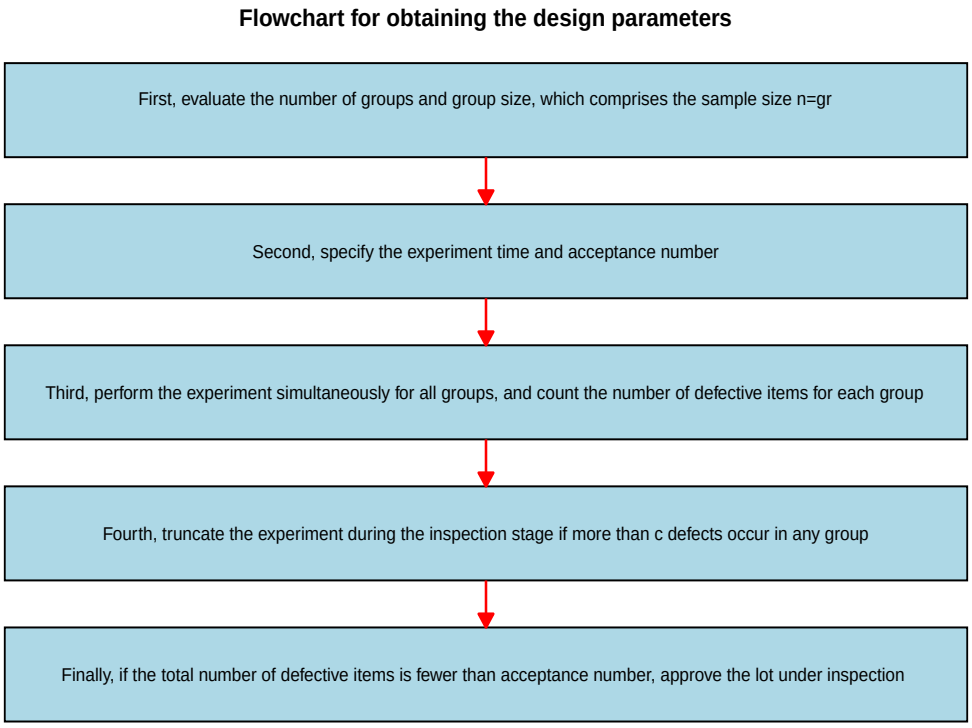

Figure 13. Flowchart for obtaining the design parameters using a GASP.

Let the product median life be m and the producer required life be m_0; then, accept the lot if $m > m_0$ at specific producer and consumer risk levels. The following formula is helpful for computing the probability of acceptance of a lot:

$$p_{a(p)} = \left[\sum_{i=0}^{c} \binom{r}{i} p^i \left[1-p\right]^{r-i}\right]^g, \tag{3.1}$$

where p is a likelihood that an item in a group fails before t_0; this may be estimated by substituting (2.14) in (2.4). However, we must first estimate the α and t. Assume $m = t_p$ in order to proceed:

$$m = \alpha \sqrt{-2\ln\left(1-\left\{-\lambda^{-1}\ln\left[1+e^{-\lambda}\ln\left(1-p\left[1-\exp\left(1-e^{\lambda}\right)\right]\right)\right]\right\}^{\frac{1}{\beta}}\right)}, \tag{3.2}$$

where t_p is given in Eq (2.14), and consider

$$\eta = \sqrt{-2\ln\left(1-\left\{-\lambda^{-1}\ln\left[1+e^{-\lambda}\ln\left(1-p\left[1-\exp\left(1-e^{\lambda}\right)\right]\right)\right]\right\}^{\frac{1}{\beta}}\right)}. \tag{3.3}$$

Now, replace $\alpha = m/\eta$, $t = a_1\, m_0$, and $r_2 = m/m_0$ in Eq (2.4). Consequently, the probability of failure

based on the EBR model can be expressed as follows:

$$W(t) = \frac{1 - \exp\left\{-e^{\lambda}\left[1 - \exp\left(-\lambda\left\{1 - \exp\left(-\frac{1}{2}\left(\frac{\eta a_1}{r_2}\right)^2\right)\right\}^{\beta}\right)\right]\right\}}{1 - \exp\{1 - e^{\lambda}\}}, \tag{3.4}$$

and p can be evaluated for a given β and λ value when r_2 and a_1 are specified. Furthermore, in order to calculate the design parameters g and c based on the operating characteristic function P_a, the following two inequalities need to be satisfied simultaneously, which are

$$p_{a\left(p_1|\frac{m}{m_0}=r_1\right)} = \left[\sum_{i=0}^{c}\binom{r}{i}p_1^i\left[1-p_1\right]^{r-i}\right]^g \leq \theta \tag{3.5}$$

and

$$p_{a\left(p_2|\frac{m}{m_0}=r_2\right)} = \left[\sum_{i=0}^{c}\binom{r}{i}p_2^i\left[1-p_2\right]^{r-i}\right]^g \geq 1-\gamma, \tag{3.6}$$

where r_1 represents the ratio at the consumer's risk, and r_2 indicates the ratio at the producer's risk. When the product lifetime follows an EBR distribution, one may compute the failure probabilities p_1 and p_2 associated with the consumer (θ) and producer (γ) risks, respectively, using Eqs (3.7) and (3.8). They are listed in the following order:

$$p_1 = \frac{1 - \exp\left\{-e^{\lambda}\left[1 - \exp\left(-\lambda\left\{1 - \exp\left(-\frac{1}{2}\left(\eta a_1\right)^2\right)\right\}^{\beta}\right)\right]\right\}}{1 - \exp\{1 - e^{\lambda}\}} \tag{3.7}$$

and

$$p_2 = \frac{1 - \exp\left\{-e^{\lambda}\left[1 - \exp\left(-\lambda\left\{1 - \exp\left(-\frac{1}{2}\left[\frac{\eta a_1}{r_2}\right]^2\right)\right\}^{\beta}\right)\right]\right\}}{1 - \exp\{1 - e^{\lambda}\}}. \tag{3.8}$$

A hypothetical example: In this section, the design parameters (g and c) for GASP are computed by considering the arbitrary parametric values $\lambda = 1$ and $\beta \in (0.5, 1.0)$, which are presented in Tables 2 and 3. Further, to estimate the effect of the EBR model's parameters on g and c, we consider four levels of true median life $r_2 \in (2, 4, 6, 8)$, two levels of $r \in (5, 10)$, four levels of consumer risk $\theta \in (0.25, 0.10, 0.05, 0.01)$, and two levels of termination ratio $a_1 \in (0.5, 1.0)$. Tables 2 and 3 display inverse functional connections between θ and g (a decrease in θ raises g). Table 3, for example, evaluates $g = 34$ for $r = 5$ and $a_1 = 0.5$, $\theta = 0.25$, and $r_2 = 2$. In the same way, $\theta = 0.10$ and $r_2 = 2$ assess $g = 560$ and subsequently $g = 729$. On the other hand, the g falls as r_2 increases. Table 3 illustrates the impact of termination ratio and r on the number of testing units. When $\theta = 0.05$, $r_2 = 2$, $a_1 = 0.5$, and $r = 5$, it shows that 2187 (729×3) units needed to be placed on a life test experiment. Similarly, the number of testing items considerably drops to 380 (95×4) when $a_1 = 1.0$ and $r = 10$ are utilized. A group size of 10 will be selected in this case because it saves substantial time and money. From Tables 2–3, the size of g decreases and the value of the operating characteristic function increases for the EBR distribution using median lifetime as the quality index. The proposed GASP based on Table 3, when $\theta = 0.05$, $r_2 = 2$, $r = 10$, and $a_1 = 1$, is as follows in Table 1:

Table 1. Proposed GASP using the EBR model.

r_2	2	4	6	8
n	70	20	10	10
g	7	2	1	1
c	5	2	1	1
$p_{(a)}$	0.9775	0.9788	0.9806	0.9934

Here, we illustrate the hypothetical case. Let us consider the following scenario: a producer believes that the product lifetime and the stated value of $m_0 = 2000$ hours follow the EBR distribution with $\lambda = \beta = 1$. Furthermore, $r = 5$, and the actual value of m equals 4000 hours, whereas the producer and consumer risks are, respectively, 0.25 and 0.050. We desire to construct a GASP for $a_1 = 0.5$, $\theta = 0.25$, and true median life $(r_2 = m/m_0) = 2$ so that we may help an experimenter who wants to do a 1000-hour life test experiment. Using Table 3 and the given information, we can use the design parameter $g = 34$ and acceptance number $c = 2$. Consequently, it is necessary to extract a sample of size 170 (34×5), with 5 units belonging to each of the 34 groups. If no more than two units in any group fail before 1000 hours, the lot is finally accepted; if more than two fail, the lot is rejected.

Table 2. GASP under the EBR model; $\lambda = 1.00$ and $\beta = 0.50$ showing minimum g and c.

		$r = 5$						$r = 10$					
		$a_1 = 0.5$			$a_1 = 1$			$a_1 = 0.5$			$a_1 = 1$		
θ	r_2	g	c	$p(a)$	g	c	$p(a)$	g	c	$p(a)$	g	c	$p(a)$
0.25	2	–	–	–	–	–	–	–	–		–	–	–
	4	8	2	0.9562	7	3	0.9783	4	3	0.9702	2	4	0.9714
	6	8	2	0.9855	3	2	0.9642	2	2	0.9653	1	3	0.9805
	8	8	2	0.9936	3	2	0.9833	2	2	0.9838	1	2	0.9517
0.10	2	–	–	–	–	–	–	–	–		–	–	–
	4	76	3	0.9807	12	3	0.963	6	3	0.9556	3	4	0.9574
	6	14	2	0.9748	4	2	0.9526	6	3	0.9890	2	3	0.9615
	8	14	2	0.9888	4	2	0.9778	3	2	0.9758	1	2	0.9817
0.05	2	–	–	–	–	–	–	–	–		–	–	–
	4	99	3	0.9750	15	3	0.9540	19	4	0.9845	7	5	0.9845
	6	18	2	0.9677	15	3	0.9890	8	3	0.9854	2	3	0.9615
	8	18	2	0.9857	5	2	0.9724	4	2	0.9678	2	3	0.9850
0.01	2	–	–	–	–	–	–	–	–		–	–	–
	4	151	3	0.9621	146	4	0.9829	29	4	0.9764	10	5	0.9779
	6	27	2	0.9520	23	3	0.9831	11	3	0.9800	5	4	0.9859
	8	27	2	0.9786	7	2	0.9615	5	2	0.9599	3	3	0.9775

Note. a large sample size is required for cells containing hyphens (–).

Table 3. GASP under the EBR model; $\lambda = 1.00$ and $\beta = 1.00$ showing minimum g and c.

		$r = 5$						$r = 10$					
		$a_1 = 0.5$			$a_1 = 1$			$a_1 = 0.5$			$a_1 = 1$		
θ	r_2	g	c	$p(a)$	g	c	$p(a)$	g	c	$p(a)$	g	c	$p(a)$
0.25	2	34	2	0.9644	7	3	0.9716	17	3	0.9844	2	4	0.9617
	4	6	1	0.9909	1	1	0.9786	2	1	0.9869	1	2	0.9894
	6	6	1	0.9981	1	1	0.9954	2	1	0.9973	1	1	0.9806
	8	2	0	0.9694	1	1	0.9985	1	0	0.9694	1	1	0.9934
0.1	2	560	3	0.9851	12	3	0.9518	27	3	0.9753	5	5	0.9839
	4	10	1	0.9849	2	1	0.9576	3	1	0.9804	1	2	0.9894
	6	10	1	0.9969	2	1	0.9908	3	1	0.9959	1	1	0.9806
	8	3	0	0.9545	2	1	0.997	3	1	0.9987	1	1	0.9934
0.05	2	729	3	0.9806	95	4	0.9842	35	3	0.9681	7	5	0.9775
	4	13	1	0.9804	2	1	0.9576	4	1	0.9739	2	2	0.9788
	6	13	1	0.9960	2	1	0.9908	4	1	0.9945	1	1	0.9806
	8	13	1	0.9988	2	1	0.997	4	1	0.9983	1	1	0.9934
0.01	2	–	–	–	146	4	0.9758	54	3	0.9513	10	5	0.9681
	4	20	1	0.9700	7	2	0.9926	6	1	0.9612	2	2	0.9788
	6	20	1	0.9938	3	1	0.9862	6	1	0.9918	2	1	0.9616
	8	20	1	0.9981	3	1	0.9954	6	1	0.9975	2	1	0.9869

4. Estimation

In statistical estimation, the value of an unknown population parameter is inferred from sample data. However, two different estimation methods, such as frequentist and Bayesian, are commonly adopted for estimation. Both methods have distinct computational frameworks; for example, in the frequentist approach, the parameter is considered fixed, whereas, in the Bayesian method, it is treated as a random variable. Moreover, the Bayesian estimation also uses some prior information to infer parameters. In this section, we use two techniques for estimating the parameters of the EBR distribution (MLE and BE).

4.1. Maximum likelihood estimation

Let $t_1, t_2, \cdots, t_n$ be the observations that follow the EBR distribution. Let $\Theta = (\alpha, \beta, \lambda)^T$ be the vector of parameters; then, the log-likelihood function of Θ is given by

$$\begin{aligned} l(\Theta) = \sum_{i=1}^{n} \ln f(t_i;\Theta) &= n\ln\lambda + n\ln\beta - 2n\ln\alpha + \sum_{i=1}^{n} t_i - 0.5\sum_{i=1}^{n}\left(\frac{t_i}{\alpha}\right)^2 \\ &+ (\beta-1)\sum_{i=1}^{n}\left(1 - e^{-0.5\left(\frac{t_i}{\alpha}\right)^2}\right) + \lambda\sum_{i=1}^{n}\left[1 - \left(1 - e^{-0.5\left(\frac{t_i}{\alpha}\right)^2}\right)^{\beta}\right] \\ &- e^{\lambda}\sum_{i=1}^{n}\left(1 - e^{-\lambda\left[1-e^{-0.5\left(\frac{t_i}{\alpha}\right)^2}\right]^{\beta}}\right) - n\ln\left[1 - \exp\left(1 - e^{\lambda}\right)\right]. \end{aligned} \tag{4.1}$$

The derivative of Eq (4.1) with respect to α, β, and λ and then set to zero yields $\hat{\alpha}, \hat{\beta}$, and $\hat{\lambda}$. In fact, there is no obvious (closed-form) solution to Eq (4.1). To get (approximate values) of the MLE estimators,

we employ quasi-Newtonian nonlinear numerical computing techniques using the AdequacyModel R package.

4.2. Bayesian estimation

Although, the posterior PDF estimation is not simple, modern computer tools (R and Python) and computational algorithms such as Markov chain Monte Carlo (MCMC) make it convenient. Assume data $t = (t_1, \cdots, t_n)$ are IID from the EBR distribution given in Eq (2.5). Suppose we wish to estimate $\Theta = (\alpha, \beta, \lambda)^T$ using the Bayesian framework. Consequently, we need the posterior PDF. It is given by

$$f(\Theta|t_1, t_2, \cdots, t_n) \propto \frac{L(t_1, t_2, \cdots, t_n|\Theta)\pi(\Theta)}{\int_{-\infty}^{+\infty} L(t_1, t_2, \cdots, t_n|\Theta)\pi(\Theta)d\Theta}, \tag{4.2}$$

where $t > 0$ is the observed data, $\Theta = (\alpha, \beta, \lambda)^T$. Let $\pi(\Theta)$ be the prior distribution of Θ, $L(t_1, t_2, \cdots, t_n|\Theta)$ be the likelihood of the data given Θ, and $f(\Theta|t_1, t_2 \cdots, t_n)$ be the posterior distribution of Θ, given data t. Then, the likelihood function can simply be obtained using Eq (2.5):

$$\begin{aligned} L(\text{data}|\Theta) = &\left(\frac{\lambda\beta}{\alpha^2}\right)^n \prod_{i=1}^{n} t_i\, e^{-0.5\sum_{i=1}^{n}\left(\frac{t_i}{\alpha}\right)^2} \prod_{i=1}^{n}\left(1 - e^{-0.5\left(\frac{t_i}{\alpha}\right)^2}\right)^{\beta-1} e^{\lambda\sum_{i=1}^{n}\left[1-\left(1-e^{-0.5\left(\frac{t_i}{\alpha}\right)^2}\right)^{\beta}\right]} \\ &\times \exp\left(-e^{\lambda}\sum_{i=1}^{n}\left\{1 - e^{-\lambda\left(1-e^{-0.5\left(\frac{t_i}{\alpha}\right)^2}\right)^{\beta}}\right\}\right)\left[1 - \exp\left(1 - e^{\lambda}\right)\right]^{-n}. \end{aligned} \tag{4.3}$$

Gamma priors are chosen for modeling scale and shape parameters because of their support for the positive real line and their capacity to accept a large variety of shapes. Moreover, gamma priors have flexibility and conjugacy properties in a wide range of lifetime and reliability models [37]. The prior is specified as

$$\pi(\alpha) = \frac{b^a}{\Gamma(a)}\alpha^{a-1}e^{-b\alpha}, \pi(\beta) = \frac{b^a}{\Gamma(a)}\beta^{a-1}e^{-b\beta}, \text{ and } \pi(\lambda) = \frac{b^a}{\Gamma(a)}\lambda^{a-1}e^{-b\lambda}. \tag{4.4}$$

Hence, using Eqs (4.3) and (4.4), the posterior PDF is as follows:

$$f(\Theta|\text{data}) = \frac{L(\text{data}|\Theta)\pi(\alpha), \pi(\beta)\pi(\lambda)}{\int\int\int L(\text{data}|\Theta)\pi(\alpha)\pi(\beta)\pi(\lambda)d\alpha\, d\beta\, d\lambda}. \tag{4.5}$$

The Metropolis–Hastings (MH) method and the Gibbs sampling technique [38, 39] with the help of the R programming language are used for Bayes estimators. The highest posterior density credible interval for $\hat{\Theta}$ is determined using the HDInterval R package [40]. To perform the MH algorithm, the following steps are employed as follows:

(i) Set up initial values of the parameters $\Theta^{(0)} = (\alpha^{(0)}, \beta^{(0)}, \lambda^{(0)})$.

(ii) Select proposal distributions (creates potential values for the parameter, for example, a new α' suggested by the existing α). Here, we choose a normal distribution and truncate it to keep positive values. They are as follows:

$$\alpha^* \sim N(\alpha^{(j)}, \sigma_\alpha^2),\ \beta^* \sim N(\beta^{(j)}, \sigma_\beta^2) \text{ and } \lambda^* \sim N(\lambda^{(j)}, \sigma_\lambda^2). \tag{4.6}$$

(iii) Compute acceptance ratio:

$$r = \frac{f(\alpha^*, \beta^*, \lambda^*|t)}{f(\alpha^{(j)}, \beta^{(j)}, \lambda^{(j)}|t)}. \tag{4.7}$$

(iv) Decides whether to keep the proposed parameter new value or stay with the previous one: generate $u \sim Uniform(0, 1)$ if $u < \min(1, r)$, then $\Theta^{(j+1)} = \Theta^*$, which means accept the new value.

Otherwise, if $u \geq \min(1, r)$, reject the proposal and keep the current value $\Theta^{(j+1)} = \Theta^{(j)}$. Finally, repeat for $J = 1000$ iterations and discard burn-in, as the early samples in the chain may not represent the posterior distribution. Consequently, the posterior mean under the squared error loss after burn-in is given by

$$\hat{\Theta} = \frac{1}{J - B} \sum_{j=B+1}^{J} \Theta^{(j)},$$

where J is the total number of MCMC iterations, B is the burn-in samples, and $\Theta^{(j)}$ is a posterior sample at iteration i.

5. Simulation

A simulation analysis holds a key position in many social and scientific experiments. In essence, it is a computational technique that models and assesses complicated systems by simulating their behavior over time under various conditions. However, Monte Carlo simulation and MCMC are highly sophisticated methods and frequently adopted due to computer computational support. Both techniques depend on generating large numbers of random samples to approximate distributions or predict the behavior of the parameters considering different sample sizes. In Bayesian statistics, for example, MCMC is used to draw a sample using posterior distribution; otherwise, it is difficult. In addition, $N = 1000$ samples of size $n = 25, 50, 100, 150, 200, 250, 300, 350, 400$ are generated using a random variable that corresponds to the EBR distribution. The following steps are considered to perform a simulation analysis:

(i) First, step up the initial parametric values for both estimation methods to generate n. Here, we examine three distinct parametric combinations: set-I = $\alpha = 0.80, \lambda = 0.90, \beta = 0.40$; set-II = $\alpha = 1.15, \lambda = 0.76, \beta = 1.20$; and set-III = $\alpha = 1.15, \lambda = 1.76, \beta = 0.50$.

(ii) In the second step, random samples are obtained using the QF given in Eq (2.14) for MLE. It is as follows:

```
q_t <- function(n, alpha, lambda, beta) {
  p <- runif(n)
  inner <- -1/lambda * log(1 + exp(-lambda) * log(1 -
    p * (1 - exp(1 - exp(lambda)))))
  alpha * sqrt(-2 * log(1 - (inner)^(1/beta)))
}
q_t(5, 1.5, 1.8, 1.2)

## [1] 0.2306223 0.6867215 0.5972751 1.0359110 0.1588109
```

Similarly, we use the MH algorithm to generate samples using the posterior PDF as briefly discussed in subsection 4.2. We use weakly informative gamma priors for α, β, and λ to guarantee that the parameters stay positive and prevent unrealistic values. The MCMC chain begins with MLE estimates. The proposal standard deviation is 15% of the MLE value.

(iii) The next step is to use the following formulas to determine the absolute biases (Abias) and mean square error (MSE) of the estimates. They are as follows:

$$\text{Abias}_{\Theta} = \left| \frac{1}{1000} \sum_{i=1}^{1000} \left(\Theta_i - \hat{\Theta}_i \right) \right| \text{ and } \text{MSE}_{\Theta} = \frac{1}{1000} \sum_{i=1}^{1000} \left(\Theta_i - \hat{\Theta}_i \right)^2, \tag{5.1}$$

where $\Theta \in (\alpha, \beta, \lambda)$, Θ_i, and $\hat{\Theta}_i$ represent the true and estimated parameters, respectively. The coverage probability (CP) is given by

$$\text{CP}_h = \frac{1}{1000} \sum_{i=1}^{1000} I(\hat{h}_i \pm 1.96 \times SE_{\hat{h}}), \tag{5.2}$$

where $I(\cdot)$ is the indicator function, and $SE_{\hat{\Theta}_i} = (SE_{\hat{\alpha}_i}, SE_{\hat{\beta}_i}, SE_{\hat{\lambda}_i})$ represents the MLEs' standard errors, which are determined by taking the inverse of the observed information matrix.

(iv) Replicate steps (ii) and (iii) $N = 1000$ times.

In general, the simulation analysis shows that under both estimation approaches, Abias and MSEs decrease as n increases. Moreover, the estimated parameters get closer to the corresponding true values (as shown in Tables 4–6). The analysis results reveal that both estimators are consistent, that is, $\hat{\Theta}_{\text{MLE}} \xrightarrow{p} \Theta$ and $\hat{\Theta}_{\text{BE}} \xrightarrow{p} \Theta$ as $n \to \infty$. The decreasing trends in absolute bias and MSE confirm asymptotic efficiency, and $\sqrt{n}(\hat{\Theta}_{\text{MLE}} - \Theta) \xrightarrow{d} \mathcal{N}(0, I^{-1}(\Theta))$. For small samples, the Bayesian estimator is influenced by the prior $\pi(\Theta)$, leading to higher variability. However, as n increases, $\pi(\Theta|x) \approx \mathcal{N}(\hat{\Theta}_{\text{MLE}}, I^{-1}(\Theta)/n)$, and both estimators perform well. The CP of the estimates approaches the 95% nominal threshold. This illustrates the usefulness of the proposed EBR distribution.

Table 4. Simulation output summary of set-I.

		MLE				BE			
Θ	n	Mean	Abias	MSE	$CP_{95\%}$	Mean	Abias	MSE	$CP_{95\%}$
	50	0.8923	0.1830	0.0606	0.9500	4.2565	3.4724	18.3598	0.8500
	100	0.8175	0.1407	0.0260	0.8500	4.1784	3.3870	16.6386	0.8500
$\alpha = 0.80$	200	0.7528	0.1011	0.0145	0.8000	1.7753	1.0147	4.6756	0.8500
	300	0.8265	0.0679	0.0091	0.9500	1.5495	0.7626	4.8565	0.9000
	500	0.8180	0.0714	0.0078	0.9000	0.9122	0.0175	0.0123	0.9500
	50	0.8920	0.2991	0.1311	1.0000	1.7773	0.9626	1.0638	0.8000
	100	0.8498	0.2142	0.0846	0.9500	1.8186	1.0026	1.1377	0.8000
$\lambda = 0.90$	200	0.7591	0.1830	0.0670	0.8500	1.1892	0.3944	0.3399	0.8000
	300	0.9045	0.1266	0.0297	0.9000	0.9160	0.0307	0.0206	0.9500
	500	0.9382	0.0922	0.0139	0.9500	0.9047	0.0149	0.0512	0.9000
	50	0.3952	0.0565	0.0045	1.0000	0.4331	0.0471	0.0035	0.9500
	100	0.4017	0.0417	0.0029	0.9500	0.4394	0.0570	0.0043	0.9100
$\beta = 0.40$	200	0.3827	0.0366	0.0018	1.0000	0.4097	0.0327	0.0016	0.9500
	300	0.3948	0.0268	0.0010	0.9500	0.4084	0.0288	0.0012	0.9500
	500	0.4052	0.0139	0.0003	0.9500	0.4115	0.0163	0.0005	0.9500

Table 5. Simulation output summary of set-II.

		MLE				BE			
Θ	n	Mean	Abias	MSE	$CP_{95\%}$	Mean	Abias	MSE	$CP_{95\%}$
	50	1.2256	0.2155	0.0876	1.0000	1.2476	0.1629	0.0459	1.0000
	100	1.0661	0.1663	0.0341	0.8000	1.1347	0.1141	0.0213	1.0000
$\alpha = 1.15$	200	1.1315	0.1283	0.0227	0.8500	1.1748	0.1292	0.0233	1.0000
	300	1.1044	0.1089	0.0166	0.8000	1.2412	0.2099	0.1283	0.9500
	500	1.1518	0.0691	0.0073	0.9500	1.1729	0.0802	0.0114	1.0000
	50	0.7907	0.3449	0.1800	1.0000	0.7547	0.1710	0.0396	1.0000
	100	0.5812	0.3610	0.1758	1.0000	0.6874	0.1312	0.0469	1.0000
$\lambda = 0.76$	200	0.6725	0.2483	0.0818	1.0000	0.6947	0.1031	0.0427	1.0000
	300	0.6180	0.2227	0.0783	1.0000	0.7092	0.0923	0.1097	0.9000
	500	0.7264	0.1835	0.0508	0.9500	0.7568	0.0210	0.0528	0.9000
	50	1.2497	0.1252	0.0317	1.0000	1.2134	0.1076	0.0208	0.9500
	100	1.1958	0.1108	0.0235	1.0000	1.2034	0.0932	0.0167	0.9000
$\beta = 1.2$	200	1.2237	0.1033	0.0149	1.0000	1.2092	0.0977	0.0127	1.0000
	300	1.1754	0.0557	0.0051	1.0000	1.1640	0.0508	0.0049	1.0000
	500	1.1760	0.0679	0.0073	0.9500	1.1663	0.0688	0.0075	0.9500

Table 6. Simulation output summary of set-III.

		MLE				BE			
Θ	n	Mean	Abias	MSE	$CP_{95\%}$	Mean	Abias	MSE	$CP_{95\%}$
	50	5.6466	6.0906	8.4639	0.5500	11.6886	11.0036	829.4802	0.6500
	100	3.7710	1.2857	4.7115	0.7211	9.0364	8.2712	333.2426	0.6500
$\alpha = 1.15$	200	1.9022	0.3403	0.3304	0.8789	3.4496	2.7907	91.1664	0.7000
	300	1.9462	0.1308	0.0713	0.9500	1.1690	0.0744	0.0860	0.9500
	500	1.1465	0.0332	0.0242	0.9500	1.1520	0.0287	0.0128	0.9500
	50	2.0412	0.7590	1.5325	0.8750	1.8877	0.7029	1.1005	0.7500
	100	2.0738	0.8270	1.4968	0.8650	2.0624	0.6840	1.2316	0.7500
$\lambda = 1.76$	200	1.7360	0.0564	0.1781	0.8789	1.7512	0.4587	0.5318	0.7000
	300	1.7097	0.0417	0.0406	0.9295	1.7288	0.0315	0.0899	0.9500
	500	1.7595	0.0167	0.0574	0.8947	1.7562	0.0175	0.0579	0.9500
	50	0.5046	0.0425	0.0030	1.0000	0.4869	0.0429	0.0029	1.0000
	100	0.5009	0.0260	0.0013	1.0000	0.4933	0.0265	0.0014	0.9500
$\beta = 0.50$	200	0.5025	0.0306	0.0014	0.9000	0.5015	0.0315	0.0014	0.9500
	300	0.4972	0.0170	0.0005	0.9500	0.4963	0.0180	0.0005	0.9500
	500	0.4946	0.0155	0.0003	0.9500	0.4918	0.0146	0.0003	0.9500

6. Practical insights

This section presents the empirical efficacy of the proposed EBR distribution considering the real-life data. The analysis addresses two key objectives: (1) highlighting the model's adaptability in identifying complex data patterns, and (2) demonstrating its interpretive worth to practitioners. To this end, we employ two real datasets.

The first dataset centers on the breaking point of fibers. The exact breaking stress depends on the fiber grade, manufacturing process, defects, and test conditions. Carbon fibers are very strong in tension but brittle and weaker than other materials in compression and shear. The breaking stress

(tensile strength) of carbon fibers is much higher than that of most engineering materials. The relevant dataset ($D1$) comprises 50 observed values measured in gigapascals (GPa), which indicate the breaking stress of carbon fibers [22]. The data are as follows: 1.12, 0.17, 0.64, 4.32, 1.22, 0.37, 1.16, 1.42, 0.09, 1.67, 0.13, 0.25, 0.08, 0.04, 2.35, 0.20, 0.78, 0.34, 1.02, 0.17, 1.76, 2.39, 0.50, 1.35, 3.36, 0.45, 0.90, 2.92, 6.53, 1.62, 7.46, 3.19, 2.49, 1.40, 7.49, 0.57, 0.14, 0.63, 5.23, 0.71, 0.68, 0.12, 0.09, 3.47, 5.93, 1.82, 4.20, 7.29, 3.13, and 3.41. The data exhibit right-skewness (skewness = 1.325) and heavy tails (kurtosis = 3.803), making them suitable for testing the EBR's capacity to model non-Gaussian phenomena. Figures 14 and 15 present a graphic illustration of $D1$ and $D2$, respectively.

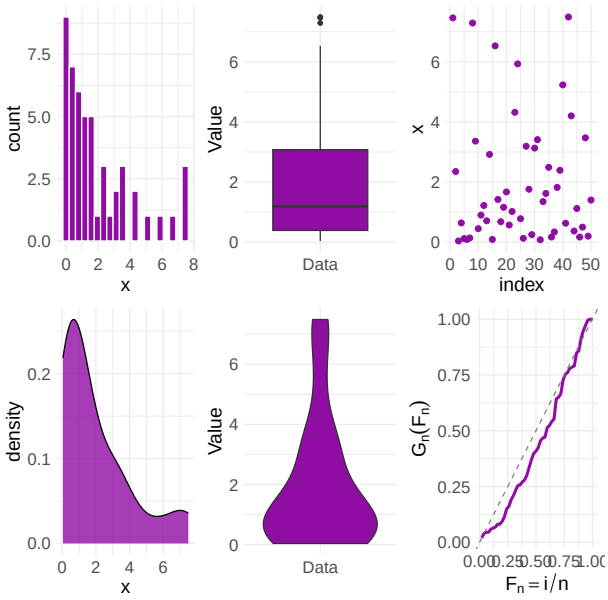

Figure 14. A visual insights of $D1$.

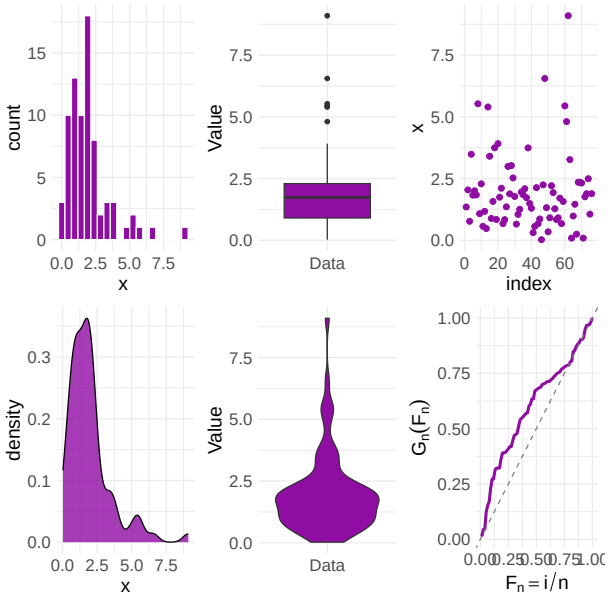

Figure 15. A visual insights of $D2$.

The second dataset focuses on the resilience of Kevlar epoxy composites. The time-to-failure data of Kevlar 373/epoxy composites, which is based on experimental observations, are used in engineering materials and reliability analysis to study the longevity behavior and durability of fiber-reinforced polymer composites under extended loading or environmental conditions. Kevlar/epoxy systems are widely utilized in aircraft structures, ballistic protection, pressure vessels, marine components, and high-performance automotive parts when long-term mechanical endurance is essential. By examining time-to-failure, engineers can forecast service life, assess material degradation, and estimate failure risk using probabilistic models such as Weibull or Lognormal distributions. The second dataset ($D2$) represents the Kevlar 373/epoxy time to failure of 76 observations [19]. It is as follows: 0.0251, 0.0886, 0.0891, 0.2501, 0.3113, 0.3451, 0.4763, 0.5650, 0.5671, 0.6566, 0.6748, 0.6751, 0.6753, 0.7696, 0.8375, 0.8391, 0.8425, 0.8645, 0.8851, 0.9113, 0.9120, 0.9836, 1.0483, 1.0596, 1.0773, 1.1733, 1.2570, 1.2766, 1.2985, 1.3211, 1.3503, 1.3551, 1.4595, 1.4880, 1.5728, 1.5733, 1.7083, 1.7263, 1.7460, 1.7630, 1.7746, 1.8275, 1.8375, 1.8503, 1.8808, 1.8878, 1.8881, 1.9316, 1.9558, 2.0048, 2.0408, 2.0903, 2.1093, 2.1330, 2.2100, 2.2460, 2.2878, 2.3203, 2.3470, 2.3513, 2.4951, 2.5260, 2.9911, 3.0256, 3.2678, 3.4045, 3.4846, 3.7433, 3.7455, 3.9143, 4.8073, 5.4005, 5.4435, 5.5295, 6.5541, and 9.0960. The data reveals right-skewness (skewness = 1.980) and heavy tails (kurtosis = 8.161). Moreover, the both datasets are overdispersed ($\sigma^2 > \mu$). The $D2$ is more consistent as compared to $D1$. The overall analysis showed that the EBR distribution works better when looking at the Kolmogorov–Smirnov (KS) test, the Cramér–von Mises (CVM) test, and the Anderson–Darling (AD) test; a better fit usually means a higher p-value (PV) for the KS test and lower values for the AD and CVM tests (as shown in Table 7).

Table 7. A summary of the fitted distributions.

	$D1$					$D2$			
Model	CVM	AD	KS	PV	Model	CVM	AD	KS	PV
EBellR	0.0885	0.5283	0.0791	0.6989	EBellR	0.0326	0.3017	0.0620	0.9907
R	0.2086	1.2016	0.2043	0.0029	R	0.0801	0.6109	0.3641	0.0004
ER	0.2221	1.2748	0.1552	0.0460	ER	0.0710	0.5568	0.0998	0.7015
E	0.1193	0.7074	0.1663	0.0263	E	0.0366	0.3280	0.1037	0.6552
EE	0.1167	0.6937	0.0953	0.4664	EE	0.0366	0.3279	0.0669	0.9786
EW	0.1167	0.6912	0.0988	0.4217	EW	0.0341	0.3100	0.0693	0.9698
W	0.1306	0.7673	0.1099	0.2953	W	0.0344	0.3126	0.0683	0.9738

Table 8 displays the estimated values $\hat{\alpha}$, $\hat{\beta}$, and $\hat{\lambda}$ based on the MLE and BE. Moreover, Table 8 shows the standard error (SE) of the estimates using MLE, the 95% lower and upper credible intervals for BE, and the goodness-of-fit (GOF) metrics. The results indicate that both methods perform well, with MLE appearing to be slightly better than BE for $D1$ (based on the AD test as $0.30165 < 0.32460$) whereas for $D2$, the BE performs better as compared to MLE (based on the AD test as ($0.51073 < 0.52835$).

Table 8. A summary of the estimated parameters and GOF measures of $D1$ and $D2$, respectively.

$D1$						
MLE			BE			
Estimates		SE	Estimates		LCI	UCI
$\hat{\alpha}$	3.94115	1.05569	$\hat{\alpha}$	3.17040	2.40427	4.06365
$\hat{\beta}$	0.42351	0.07881	$\hat{\beta}$	0.52770	0.40227	0.65853
$\hat{\lambda}$	0.79069	0.40074	$\hat{\lambda}$	0.80440	0.33459	1.23337
Measures of goodness-of-fit based on $D1$						
MLE			BE			
CVM	0.03258		CVM	0.03620	–	–
AD	0.30165		AD	0.32460	–	–
KS	0.06200		KS	0.10933	–	–
PV	0.99070		PV	0.55170	–	–
$D2$						
MLE			BE			
Estimates		SE	Estimates		LCI	UCI
$\hat{\alpha}$	4.21236	2.5112	$\hat{\alpha}$	3.93769	2.45903	5.92155
$\hat{\beta}$	0.81344	0.0870	$\hat{\beta}$	0.86968	0.68578	1.03054
$\hat{\lambda}$	1.48049	0.5864	$\hat{\lambda}$	1.42976	0.90338	1.95061
Measures of goodness-of-fit based on $D2$						
MLE			BE			
CVM	0.08849		CVM	0.08589	–	–
AD	0.52835		AD	0.51073	–	–
KS	0.07907		KS	0.10415	–	–
PV	0.69890		PV	0.35700	–	–

Because the AD test is more powerful than the KS test, we use it to compare the two estimation methods. Moreover, Table 9 also supports Table 8. Recently, the Marshall–Olkin–Kumaraswamy exponential (MOKE) distribution was used by Almarashi et al. [22] to develop a GASP using carbon fiber breaking strength data. Moreover, they provided a goodness-of-fit measure of $KS = 0.0681$ with $PV = 0.9743$. Tables 10 and 11 provide the GASP based on the MLE and BE of $D1$. The overall results demonstrate that the BE lowers the design parameter g, which lowers the experiment's cost and duration.

Table 9. A summary of log-likelihood ($\hat{\ell}$), Akaike information criterion (AIC), and Bayesian information criterion (BIC) of $D1$ and $D2$, respectively.

	$D1$			$D2$		
	$-\hat{\ell}$	AIC	BIC	$-\hat{\ell}$	AIC	BIC
MLE	82.8436	171.6872	177.4233	121.3181	248.6362	255.6284
BE	95.8575	197.7150	203.4511	123.1679	252.3357	259.3279

Table 10. A GASP based on the MLE ($\hat{\alpha} = 3.94115, \hat{\beta} = 0.42351, \hat{\lambda} = 0.79069$) and BE ($\hat{\alpha} = 3.1704, \hat{\beta} = 0.5277, \hat{\lambda} = 0.8044$) estimators of $D1$, taking $r = 5$.

							$r = 5$						
		MLE			**BE**			**MLE**			**BE**		
		$a_1 = 0.5$			$a_1 = 0.5$			$a_1 = 1.0$			$a_1 = 1.0$		
θ	r_2	g	c	$p(a)$	g	c	$p(a)$	g	c	$p(a)$	g	c	$p(a)$
0.25	2	–	–	–	–	–	–	–	–		–	–	–
	4	36	3	0.9745	9	2	0.9663	7	3	0.9601	7	3	0.9846
	6	39	2	0.9679	9	2	0.9898	7	3	0.9879	3	2	0.9742
	8	7	2	0.9836	3	1	0.9624	3	2	0.9650	1	1	0.9514
0.10	2	–	–	–	–	–	–	–	–		–	–	–
	4	59	3	0.9586	89	3	0.9866	73	4	0.9809	12	3	0.9737
	6	59	3	0.9883	15	2	0.9831	12	3	0.9794	4	2	0.9657
	8	11	2	0.9743	4	1	0.9501	4	2	0.9536	4	2	0.9849
0.05	2	–	–	–	–	–	–	–	–		–	–	–
	4	904	4	0.9842	116	3	0.9826	95	4	0.9753	15	3	0.9672
	6	77	3	0.9848	20	2	0.9775	15	3	0.9743	5	2	0.9573
	8	15	2	0.9651	20	2	0.9905	15	3	0.9893	5	2	0.9811
0.01	2	–	–	–	–	–	–	–	–		–	–	–
	4				178	3	0.9735	146	4	0.9622	23	3	0.9501
	6	117	3	0.9769	30	2	0.9664	23	3	0.9609	23	3	0.9893
	8	117	3	0.9908	30	2	0.9857	23	3	0.9837	7	2	0.9737

Table 11. A GASP based on the MLE ($\hat{\alpha} = 3.94115, \hat{\beta} = 0.42351, \hat{\lambda} = 0.79069$) and BE ($\hat{\alpha} = 3.1704, \hat{\beta} = 0.5277, \hat{\lambda} = 0.8044$) estimators of $D1$, taking $r = 10$.

							$r = 10$						
		MLE			**BE**			**MLE**			**BE**		
		$a_1 = 0.5$			$a_1 = 0.5$			$a_1 = 1.0$			$a_1 = 1.0$		
θ	r_2	g	c	$p(a)$	g	c	$p(a)$	g	c	$p(a)$	g	c	$p(a)$
0.25	2	–	–	–	37	5	0.9502	–	–	–	–	–	–
	4	7	4	0.9810	4	3	0.9815	3	5	0.9845	2	4	0.9501
	6	3	3	0.9821	2	2	0.9775	1	3	0.9595	1	3	0.9870
	8	2	2	0.9559	2	2	0.9900	1	3	0.9811	1	2	0.9657
0.1	2	–	–	–	–	–	–	–	–	–	–	–	–
	4	12	4	0.9677	7	3	0.9678	5	5	0.9742	3	4	0.9708
	6	5	3	0.9703	3	2	0.9664	3	4	0.9778	2	3	0.9741
	8	5	3	0.9873	3	2	0.9851	2	3	0.9625	1	2	0.9657
0.05	2	–	–	–	–	–	–	–	–	–	–	–	–
	4	15	4	0.9598	8	3	0.9633	7	5	0.9641	4	4	0.9612
	6	6	3	0.9645	4	2	0.9555	4	4	0.9705	2	3	0.9741
	8	6	3	0.9847	4	2	0.9802	2	3	0.9625	2	3	0.9907
0.01	2	–	–	–	–	–	–	–	–	–	–	–	–
–	4	71	5	0.9805	34	4	0.9851	–	–	–	5	4	0.9517
	6	23	4	0.9860	13	3	0.9870	5	4	0.9632	3	3	0.9614
	8	9	3	0.9772	6	2	0.9704	5	4	0.9864	3	3	0.9861

Fayomi and Khan [19] designed a GASP using the mean as a quality parameter instead of the median. They employed Kevlar 373/epoxy fatigue fracture life data ($D2$). In addition, they applied

another generalized transmuted exponential (AGTE) distribution and found $KS = 0.0957$. We use the same set of data, and our proposed model yields an improved KS =0.07907 test value.

A GASP based on the EBR distribution taking the estimated parametric values of MLE and BE of $D2$ is presented in Tables 12 and 13.

Table 12. A GASP based on the MLE ($\hat{\alpha} = 3.94115, \hat{\beta} = 0.42351, \hat{\lambda} = 0.79069$) and BE ($\hat{\alpha} = 3.1704, \hat{\beta} = 0.5277, \hat{\lambda} = 0.8044$) estimators of $D2$, taking $r = 5$.

						$r = 5$						
		MLE			BE			MLE			BE	
		$a_1 = 0.5$			$a_1 = 0.5$			$a_1 = 1.0$			$a_1 = 1.0$	
θ	r_2	g	c	$p(a)$	g	c	$p(a)$	g	c	$p(a)$	g	c	$p(a)$
0.25	2	163	3	0.9748	205	3	0.9816	44	4	0.981	7	3	0.9536
	4	5	1	0.9697	5	1	0.9802	1	1	0.9505	1	1	0.9618
	6	5	1	0.9915	5	1	0.9950	1	1	0.9851	1	1	0.9896
	8	5	1	0.9966	5	1	0.9981	1	1	0.9939	1	1	0.9960
0.1	2	270	3	0.9586	340	3	0.9697	73	4	0.9686	73	4	0.9767
	4	7	1	0.9579	8	1	0.9685	4	2	0.9845	4	2	0.9896
	6	7	1	0.9882	8	1	0.9920	2	1	0.9704	2	1	0.9793
	8	7	1	0.9953	8	1	0.997	2	1	0.9878	2	1	0.992
0.05	2	–	–	–	442	3	0.9608	95	4	0.9594	95	4	0.9698
	4	43	2	0.9932	10	1	0.9608	5	2	0.9806	5	2	0.9870
	6	9	1	0.9848	10	1	0.9900	2	1	0.9704	2	1	0.9690
	8	9	1	0.9939	10	1	0.9962	2	1	0.9878	2	1	0.9920
0.01	2	–	–	–	–	–	–	–	–	–	146	4	0.9540
	4	66	2	0.9896	77	2	0.9937	7	2	0.9730	7	2	0.9819
	6	14	1	0.9765	16	1	0.9841	3	1	0.9560	3	1	0.9690
	8	14	1	0.9906	16	1	0.9939	2	1	0.9817	3	1	0.9881

Table 13. A GASP based on the MLE ($\hat{\alpha} = 3.94115, \hat{\beta} = 0.42351, \hat{\lambda} = 0.79069$) and BE ($\hat{\alpha} = 3.1704, \hat{\beta} = 0.5277, \hat{\lambda} = 0.8044$) estimators of $D2$, taking $r = 10$.

						$r = 10$						
		MLE			BE			MLE			BE	
		$a_1 = 0.5$			$a_1 = 0.5$			$a_1 = 1.0$			$a_1 = 1.0$	
θ	r_2	g	c	$p(a)$	g	c	$p(a)$	g	c	$p(a)$	g	c	$p(a)$
0.25	2	9	3	0.9574	3	3	0.9686	3	5	0.9739	3	5	0.9809
	4	4	2	0.9931	2	1	0.9667	1	2	0.9649	1	2	0.9756
	6	2	1	0.9854	2	1	0.9913	1	2	0.9937	1	1	0.9580
	8	2	1	0.9941	2	1	0.9967	1	1	0.9746	1	1	0.9832
0.1	2	54	4	0.9574	69	4	0.9836	5	5	0.9569	5	5	0.9683
	4	6	2	0.9897	3	1	0.9505	1	2	0.9649	1	2	0.9756
	6	3	1	0.9782	3	1	0.9870	1	2	0.9937	1	1	0.9580
	8	3	1	0.9911	3	1	0.9950	1	1	0.9746	1	1	0.9832
0.05	2	70	4	0.9682	90	4	0.9786	–	–	–	7	5	0.9559
	4	7	2	0.9880	8	2	0.9927	2	3	0.9904	2	2	0.9518
	6	3	1	0.9782	4	1	0.9827	2	2	0.9874	1	1	0.9580
	8	3	1	0.9911	4	1	0.9933	1	1	0.9746	1	1	0.9832
0.01	2	108	4	0.9514	138	4	0.9674	–	–	–		–	–
	4	11	2	0.9812	12	2	0.9891	3	3	0.9856	2	2	0.9518
	6	5	1	0.9640	5	1	0.9784	2	2	0.9874	2	2	0.9925
	8	5	1	0.9853	5	1	0.9917	2	2	0.9966	2	1	0.9667

Both estimate techniques work well; however, when r increases, the g tends to decrease rapidly. The comparative analysis is presented in Tables 14 and 15 for both $D1$ and $D2$, respectively. Generally, for $r_2 = 6$, we need to test $n = 80$ items under the MOKE model, $n = 50$ items under the EBR (MLE), and $n = 30$ items under the EBR (BE) of $D1$. This indicates a decrease in sample size under BE.

Table 14. Comparative study of a GASP, when $r = 10$, $a_1 = 1$, and $\theta = 0.01$ of $D1$.

MOKE (MLE) [22]					EBR (MLE)					EBR (BE)				
r_2	n	g	c	$p_{(a)}$	r_2	n	g	c	$p_{(a)}$	r_2	n	g	c	$p_{(a)}$
2	–	–	–	–	2	–	–	–	–	2	–	–	–	–
4	80	8	3	0.9510	4	–	–	–	–	4	50	5	4	0.9517
6	80	8	3	0.9896	6	50	5	4	0.9632	6	30	3	3	0.9614
8	40	4	2	0.9765	8	50	5	4	0.9864	8	30	3	3	0.9861

Table 15. Comparative study of a GASP, when $r = 10$, $a_1 = 1$, and $\theta = 0.25$ of $D2$.

AGTE (MLE) [19]					EBR (MLE)					EBR (BE)				
r_2	n	g	c	$p_{(a)}$	r_2	n	g	c	$p_{(a)}$	r_2	n	g	c	$p_{(a)}$
2	–	–	–	–	2	30	3	5	0.9739	2	30	3	5	0.9809
4	–	–	–	–	4	10	1	2	0.9649	4	10	1	2	0.9756
6	30	3	4	0.9547	6	10	1	2	0.9937	6	10	1	1	0.9580
8	30	3	4	0.9854	8	10	1	1	0.9746	8	10	1	1	0.9832

However, we must test $n = 30$ items under the MOKE model, $n = 10$ items under the EBR (MLE), and $n = 10$ items under the EBR (BE) of $D2$ for $r_2 = 6$. This demonstrates that, in contrast to the AGTE model, both estimating approaches perform well under the EBR model. This substantial reduction in sample size demonstrates the benefit of the proposed distribution by enhancing acceptance sampling decision-making at a low cost and accurately reflecting the underlying lifetime behavior.

The actual and estimated PDFs and CDFs of the EBR model for $D1$ and $D2$ under both estimation procedures are graphically shown in Figures 16 and 17. Both estimating techniques display good agreement between actual and estimated values. Similarly, Figure 18 presents a graphic representation of iterations based on the MH algorithm and Gibbs sampling and estimated posterior PDFs for $D1$ and $D2$. Overall, both diagnostic plots reveal that the proposed model performs efficiently under the Bayesian framework (unimodal posterior), indicating stable posterior inference and reliable parameter estimation for the given datasets. A graphic representation of the estimated probability–probability (P–P) plots using the MLE and BE for $D1$ and $D2$ is presented in Figures 19 and 20 and support the numerical findings of the EBR model. Finally, a plot of the profile log-likelihood function of the parameters α, β, and λ under the EBR model for $D1$ and $D2$ can be viewed in Figures 21 and 22. The 3D surface plots provide a clearer view of the joint's posterior structure of the estimators. A graphic illustration (as shown in Figures 23 and 24) suggests one prominent peak; the posterior distribution is unimodal. Moreover, these plots indicate robust posterior inference, good convergence, and well-behaved joint parameter distributions.

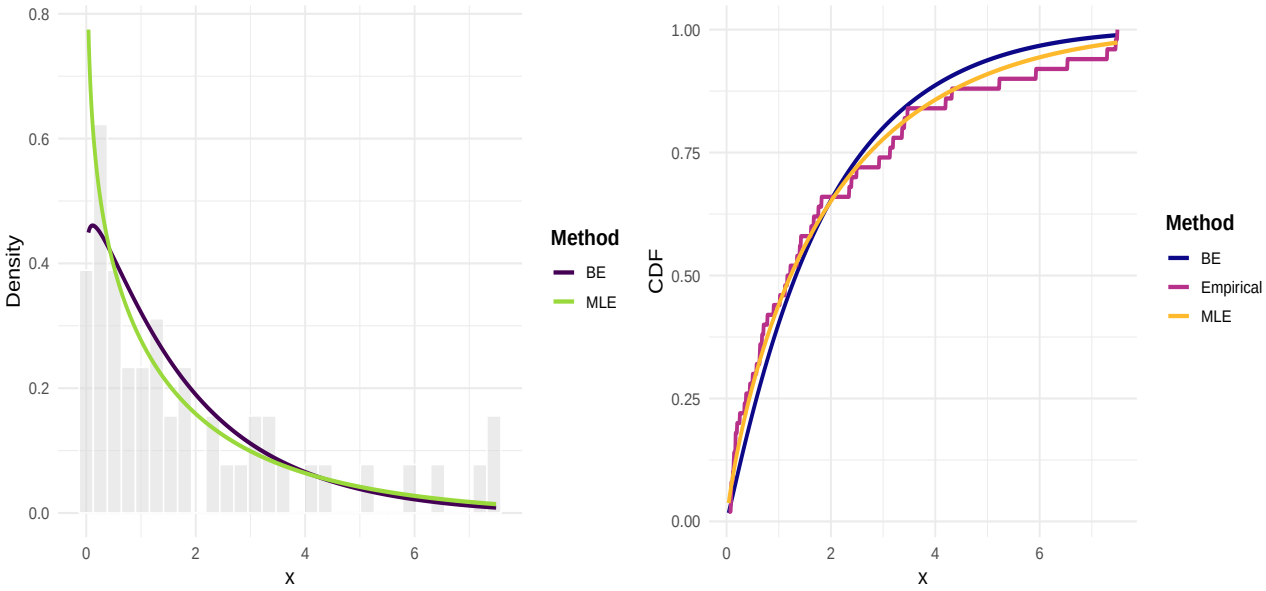

Figure 16. A graphic representation of the estimated PDF and estimated CDF based on the MLE and BE for D^I.

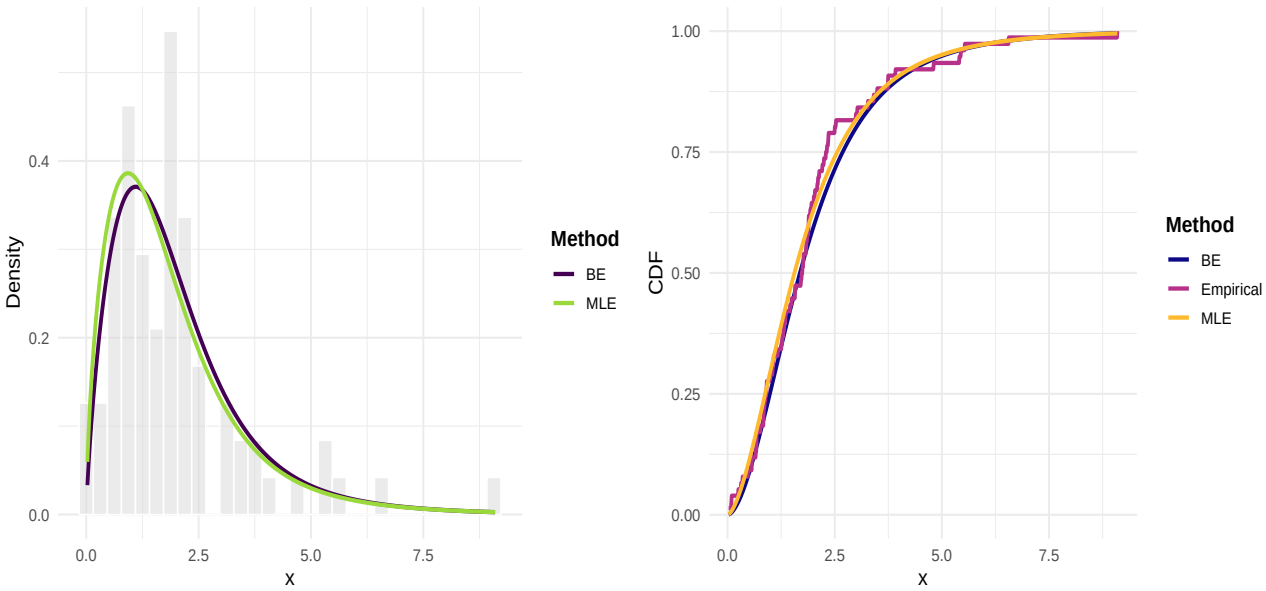

Figure 17. A graphic representation of the estimated PDF and estimated CDF based on the MLE and BE for $D2$.

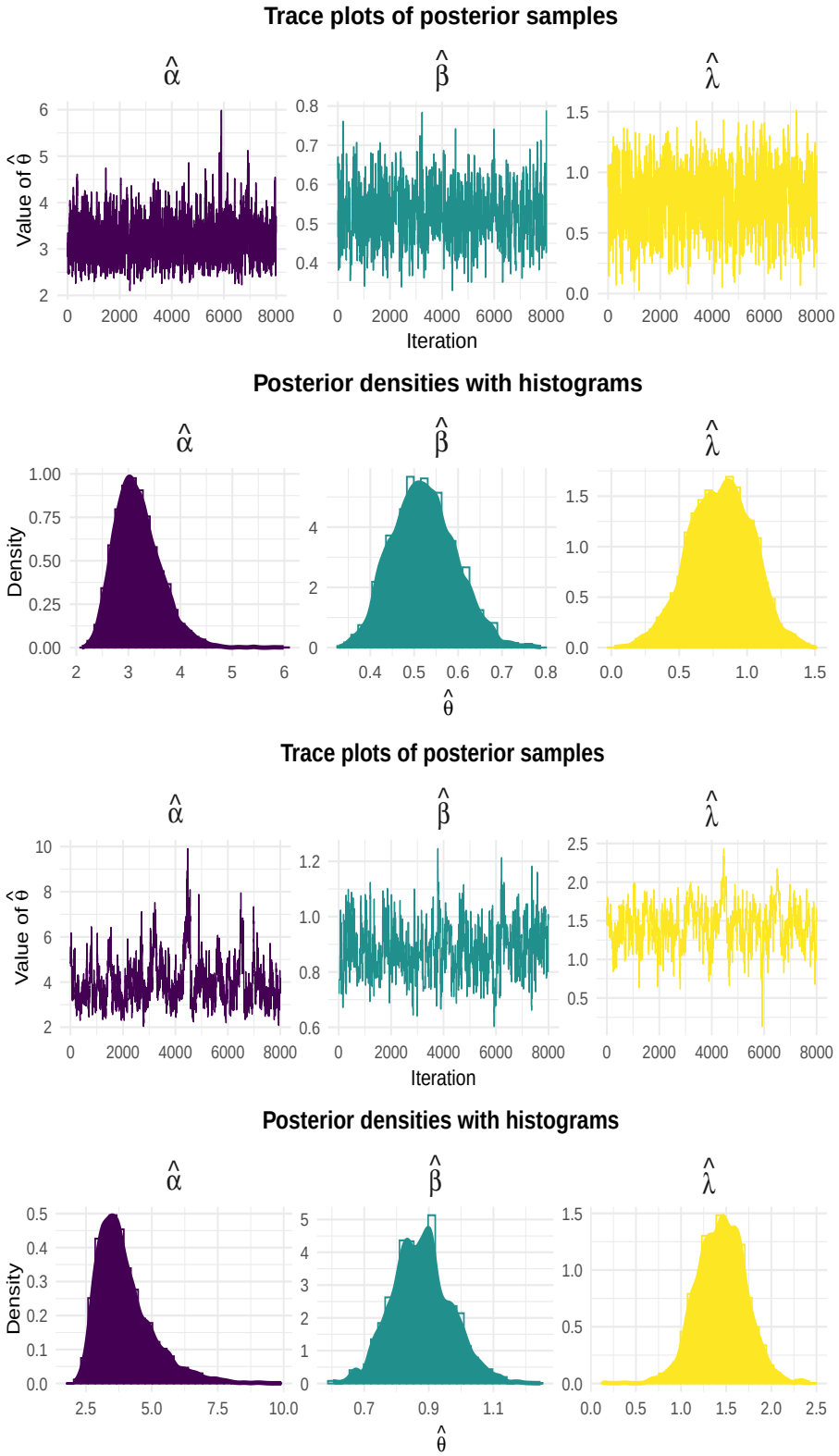

Figure 18. A graphic representation of iterations based on the MH algorithm and estimated posterior densities for $D1$ and $D2$, respectively.

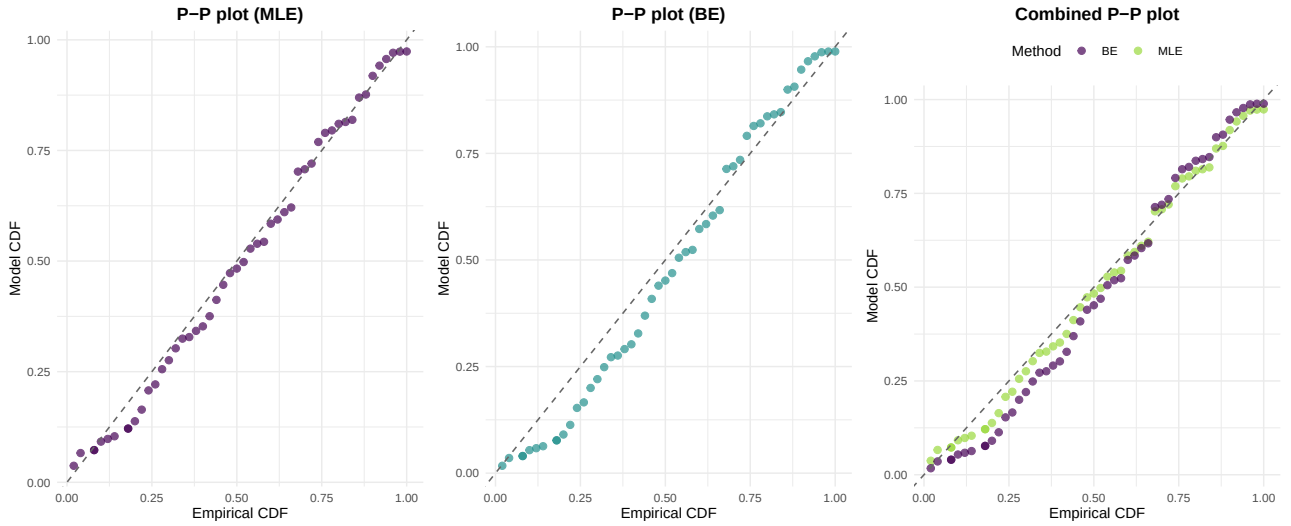

Figure 19. A graphic representation of the estimated P-P plots using the MLE and BE for $D1$.

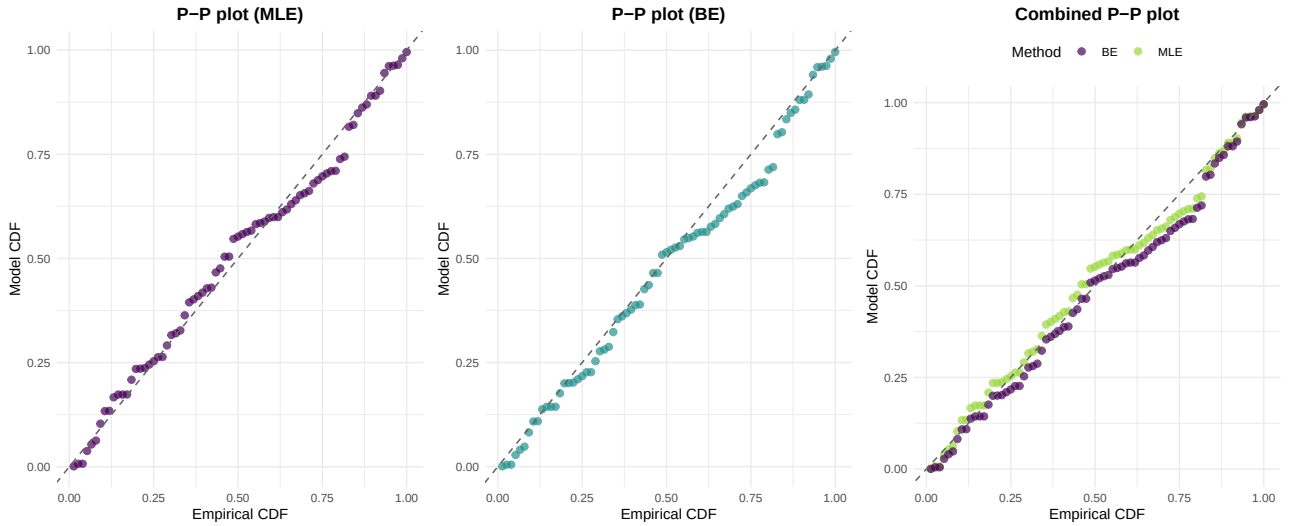

Figure 20. A graphic representation of the estimated P-P plots using the MLE and BE for $D2$.

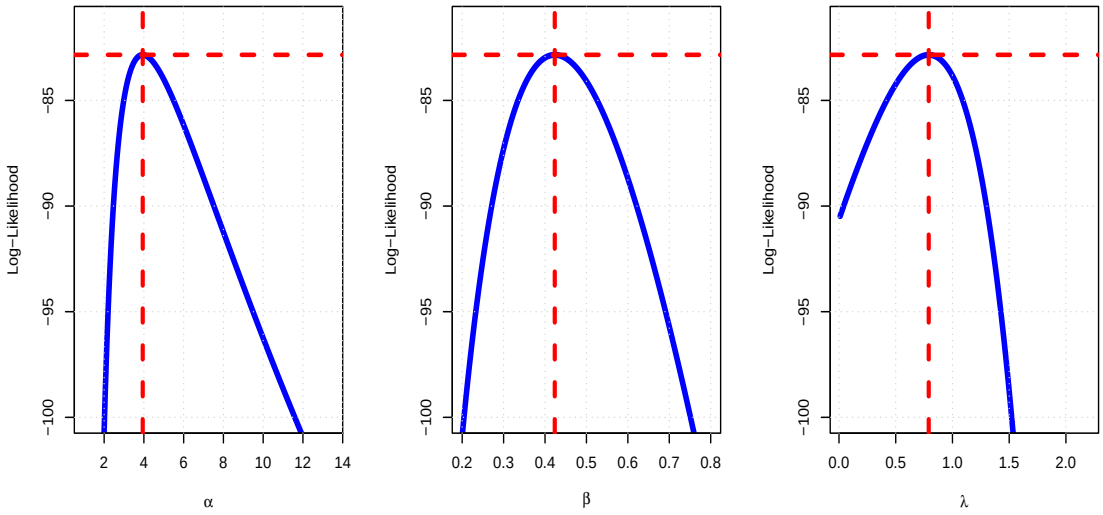

Figure 21. A plot of the profile log-likelihood function under the EBR model for $D1$.

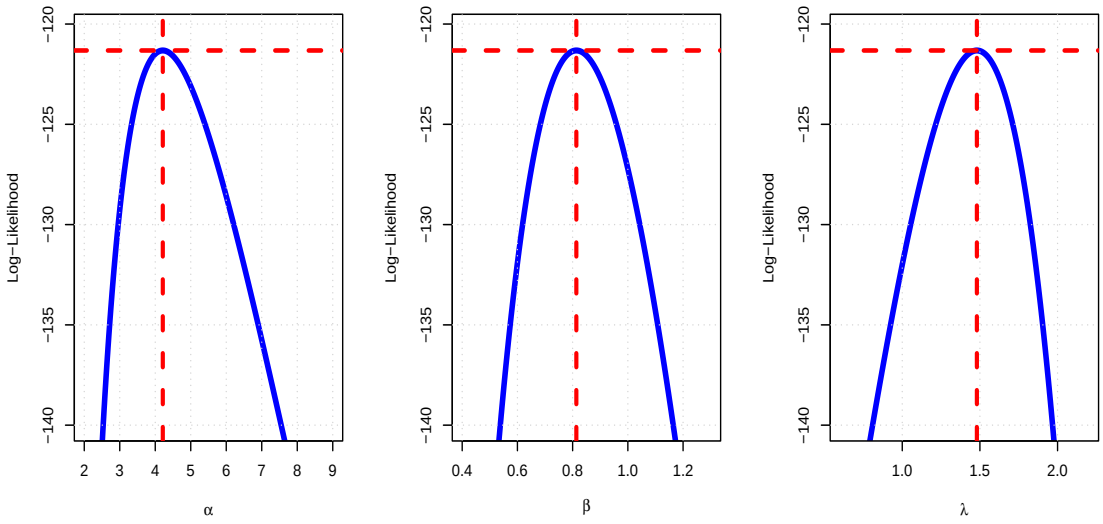

Figure 22. A plot of the profile log-likelihood function under the EBR model for $D2$.

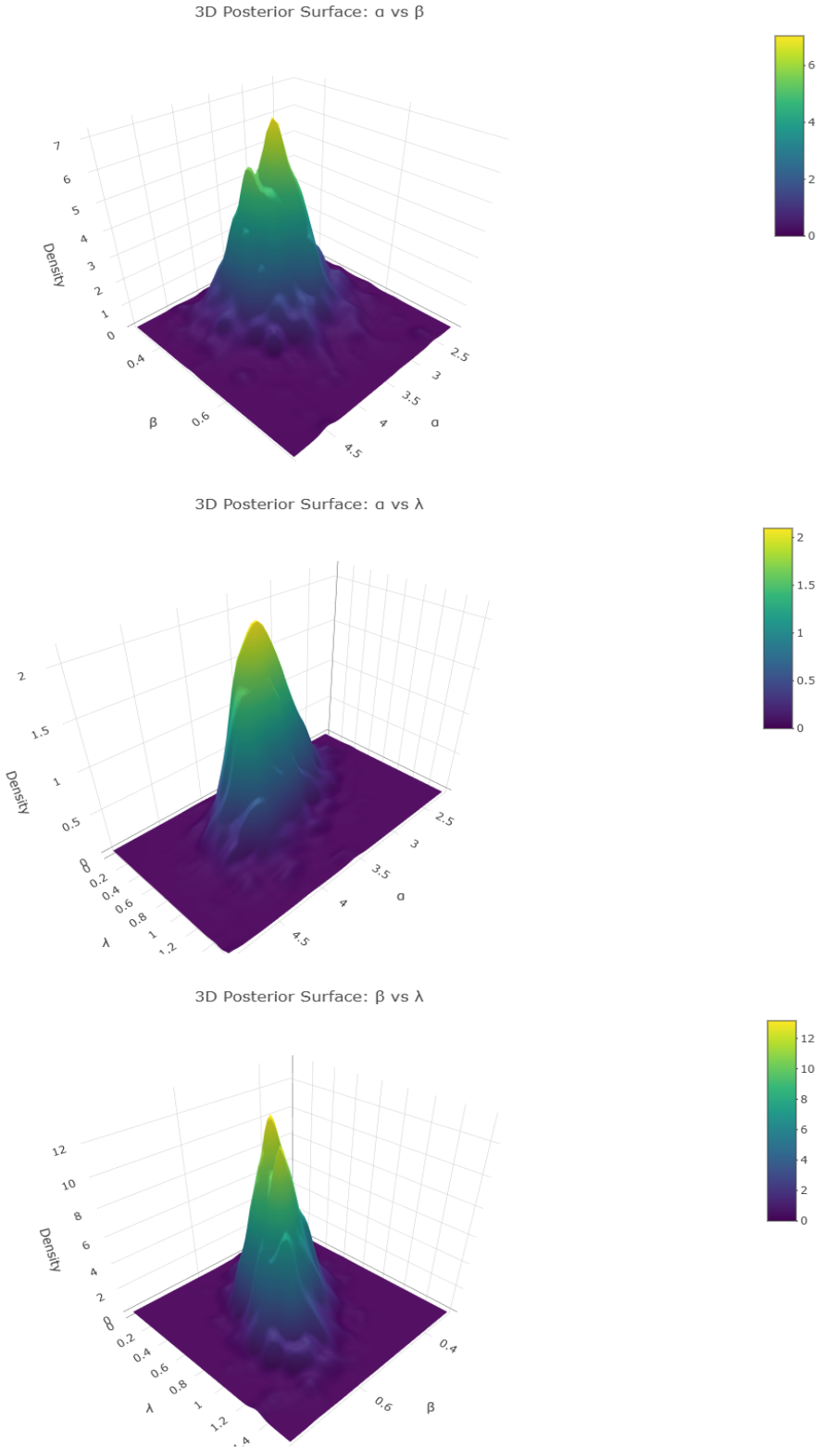

Figure 23. The 3D posterior density surface plots for D_1.

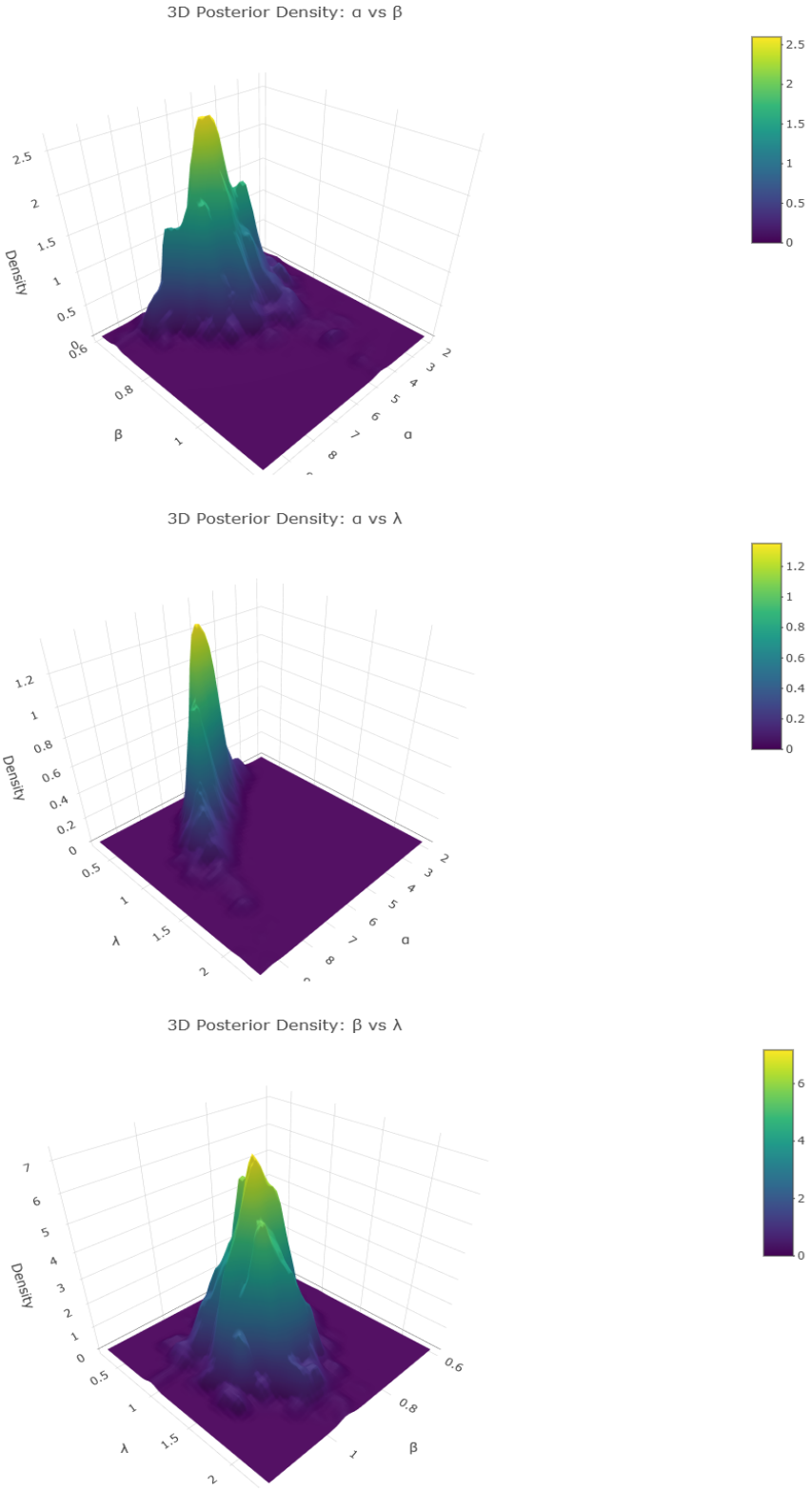

Figure 24. The 3D posterior density surface plots for D_2.

7. Censored data application

Censoring is a statistical phenomenon in which the exact value of a random variable cannot be fully observed due to experimental or observational limitations. This is common in disciplines such as survival analysis, reliability engineering, and econometrics. For instance, a clinical trial study is designed to examine how long people survive after receiving cancer treatment. At the end of the five-year trial, some patients are still living. Censoring can be left, right, and interval. Let T be a non-negative random variable indicating the true event time (e.g., time until failure or death) and C denote the censoring time [41, 42]. Then, the general censoring mechanism for the observed time $Z = \min(T, C)$ and censoring indicator are as follows:

$$\delta = \begin{cases} 1, & \text{if } T \leq C \quad \text{(event observed)}, \\ 0, & \text{if } T > C \quad \text{(right-censored)}. \end{cases} \tag{7.1}$$

Then, the observed data with censoring status (0 and 1) can be viewed as (Z_i, δ_i), $i = 1, 2, \cdots, n$. Moreover, in the presence of right censoring, the likelihood function becomes:

$$l(\Theta) = \prod_{i=1}^{76} [w(z_i; \Theta)]^{\delta_i} [1 - W(z_i; \Theta)]^{1-\delta_i}, \tag{7.2}$$

where $w(z_i; \Theta)$ and $1 - W(z_i; \Theta)$ are the PDF and survival function, respectively. Here, we use the simulated data obtained using the QF given in Eq (2.14). Multiple censoring levels (40%, 60%, and 80%) are used to examine model behavior across varying sample sizes, considering the Cox–Snell (CS) residual accuracy measure. Graphical illustrations suggest that the model is asymptotically well-behaved; its accuracy is increases as the volume of data increases (as shown in Figures 25–27). This indicates the EBR distribution's effectiveness as a reliable tool for evaluating high-integrity systems with low or severely censored data.

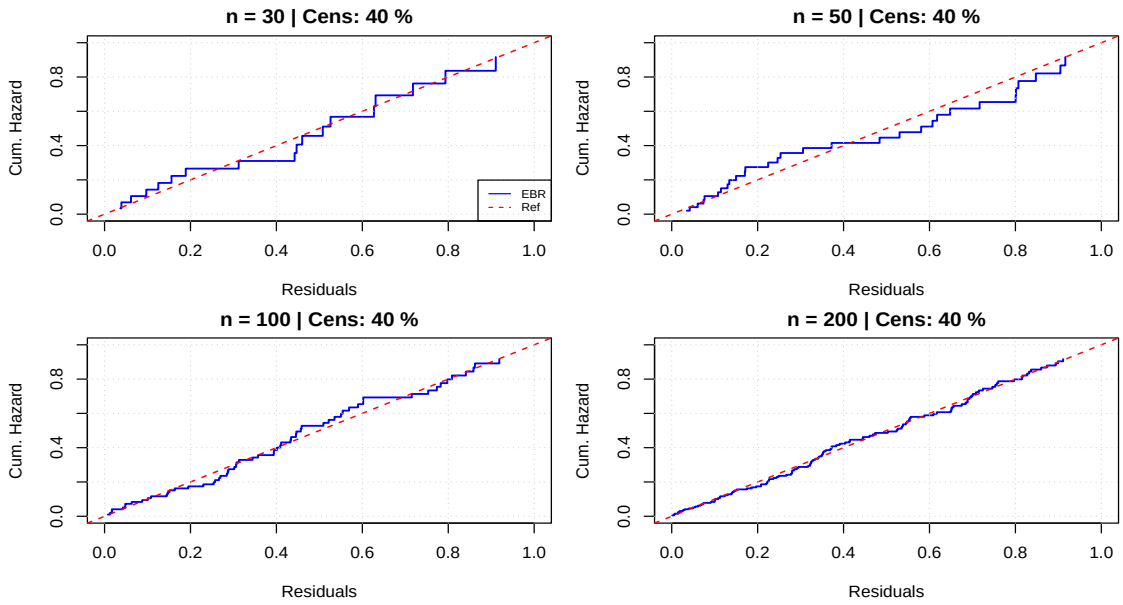

Figure 25. A graphical illustration of the CS residuals under 40% censoring for different sample sizes.

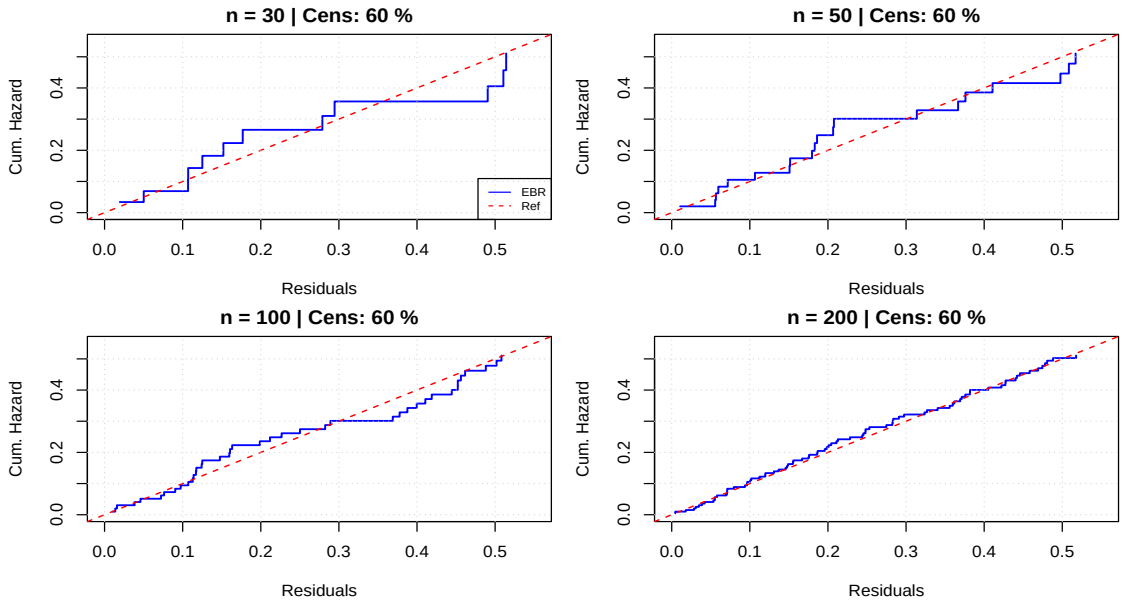

Figure 26. A graphical illustration of the CS residuals under 60% censoring for different sample sizes.

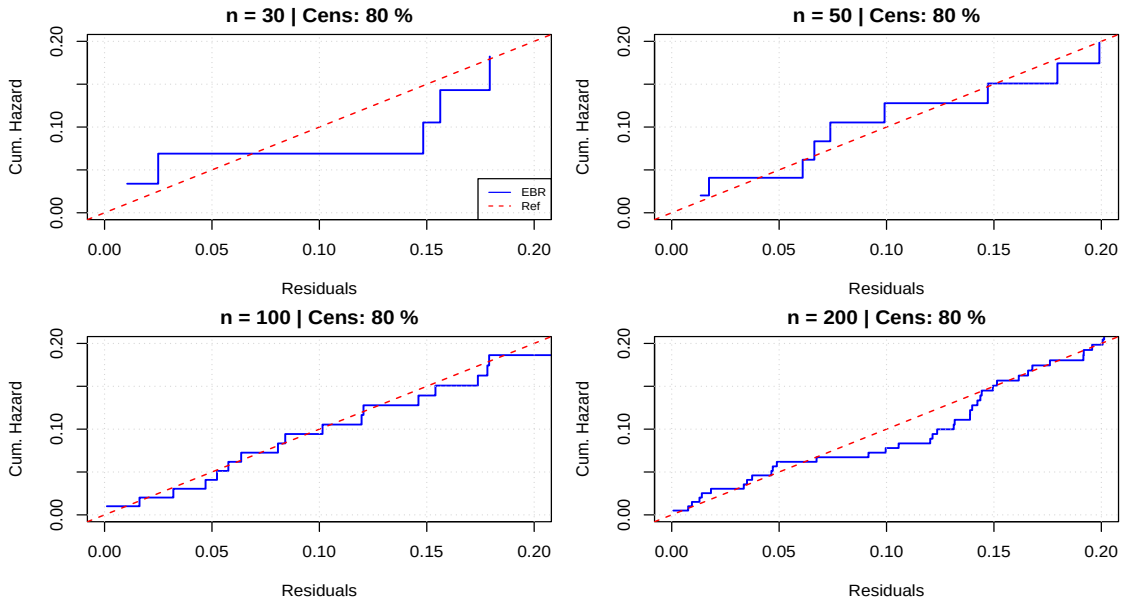

Figure 27. A graphical illustration of the CS residuals under 80% censoring for different sample sizes.

Illustration with real data: We use kidney patient survival data containing $i = 1, 2, \cdots n = 76$ observations. The data are obtained using the survival R package [43]. The data with censoring status are as follows: (8,1), (16,1), (23,1), (13,0), (22,1), (28,1), (447,1), (318,1), (30,1), (12,1), (24,1), (245,1), (7,1), (9,1), (511,1), (30,1), (53,1), (196,1), (15,1), (154,1), (7,1), (333,1), (141,1), (8,0), (96,1), (38,1), (149,0), (70,0), (536,1), (25,0), (17,1), (4,0), (185,1), (177,1), (292,1), (114,1), (22,0), (149,0), (15,1), (108,0), (152,1), (562,1), (402,1), (24,0), (13,1), (66,1), (39,1), (46,0), (12,1), (40,1),

(113,0), (201,1), (132,1), (156,1), (34,1), (30,1), (2,1), (25,1), (130,1), (26,1), (27,1), (58,1), (5,0), (43,1), (52,1), (30,1), (190,1), (5,0), (119,1), (8,1), (54,0), (16,0), (6,0), (78,1), (63,1), and (8,0). The descriptive summary by status is presented in Table 16. Figure 28 presents a graphic illustration of the survival data.

Table 16. Descriptive insights of the data by status (n=76).

Status	n	%	μ	σ	$\tilde{z}$	z_{min}	z_{max}	z_{skew}	z_{kur}
0	18	23.7	46.4	51.7	23	4	159	1.12	2.83
1	58	76.3	118.8	143.1	48	2	562	1.67	5.03
Total	76	100	101.6	130.9	39.5	2	562	1.97	6.45

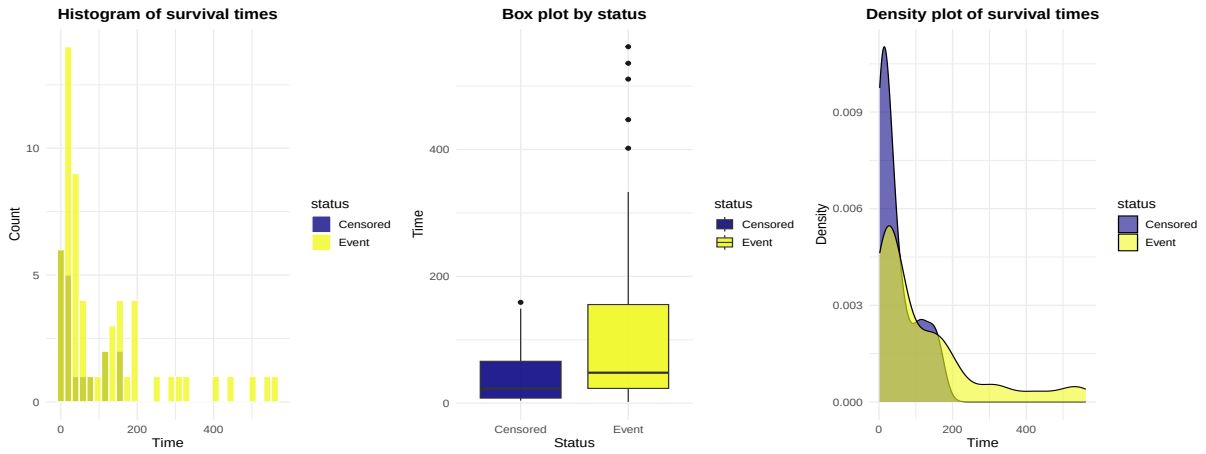

Figure 28. A status-based visual overview of the data.

Figure 29 presents a graphic overview of the KM curve with censored points and 95% confidence interval (C.I) of the data. On the other side, the fitted distributions to the data, namely the Rayleigh, ER, and EBR, are presented in Figure 30. The estimated parameters and standard errors (SE) of the estimates of the fitted distributions using MLE are shown in Table 17. The general output of the numeric and graphic analysis (see Figure 30 and the Cox–Snell residual analysis in Figure 31) support the EBR distribution (as shown in Table 18).

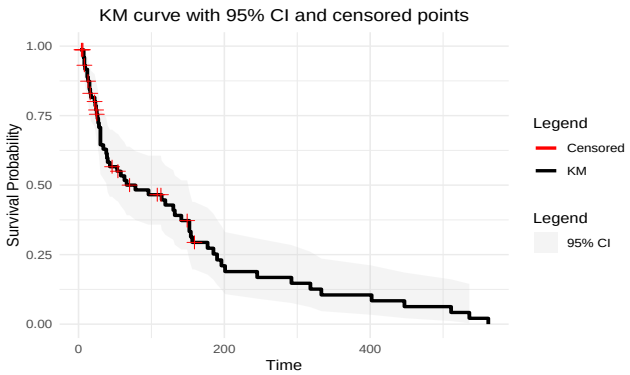

Figure 29. The KM curve with censored points and 95% C.I (n=76).

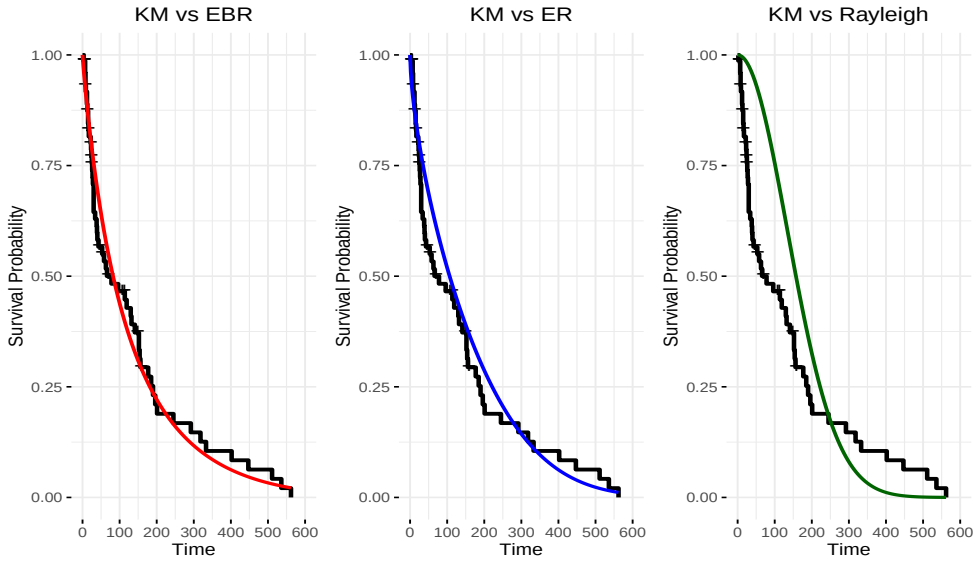

Figure 30. The KM curve over the fitted distributions of the data ($n = 76$).

Table 17. Estimated parameters and SE of the fitted distributions.

Model		EBR			ER	Rayleigh
Parameter	$\hat{\alpha}$	$\hat{\lambda}$	$\hat{\beta}$	$\hat{\alpha}$	$\hat{\beta}$	$\hat{\alpha}$
Estimate	307.981	1.0103	0.4612	217.0630	0.3188	133.5971
SE	101.819	0.3565	0.0630	28.3355	0.0426	8.7711

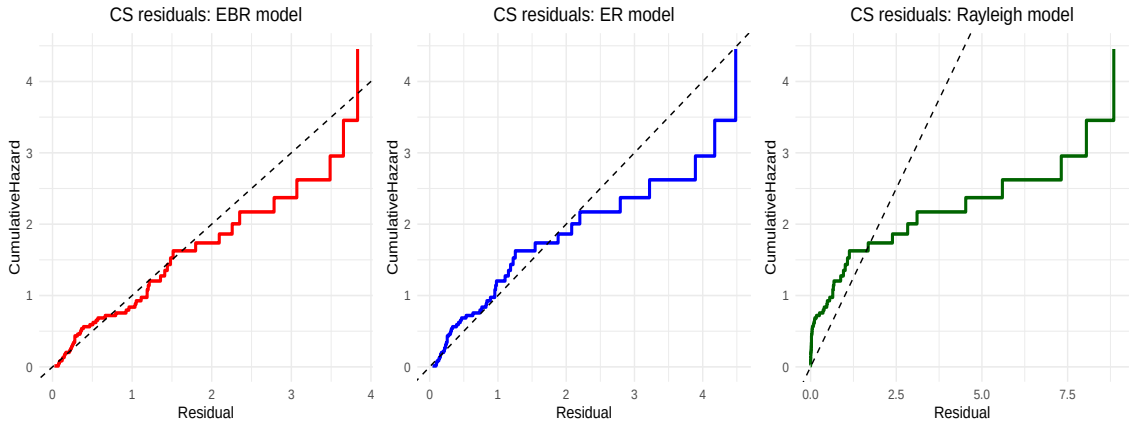

Figure 31. A graphic demonstration of the CS residual.

Table 18. Fitted distributions with GOF measures.

Model	LogLikelihood	AIC
EBR	-340.443	686.886
ER	-343.536	691.072
Rayleigh	-392.353	786.705

The estimated parameters with 95% LCI, UCI, and GOF measures using BE are presented in Tables 19 and 20. Figures 32 and 33 show the fitted EBR distribution with CS residual and trace plots and posterior PDFs of the estimated parameters. The general findings by comparing the two estimation methods for survival analysis show that MLE outperforms other metrics.

Table 19. Estimated parameters using BE with 95% LCI and UCI of the EBR distribution.

Parameter	Mean estimate	LCI	UCI
$\hat{\alpha}$	573.1570	203.7469	1707.2928
$\hat{\lambda}$	1.2068	0.2223	2.1800
$\hat{\beta}$	0.4522	0.3174	0.5690

Table 20. GOF measures using BE of the fitted EBR distribution.

LogLikelihood	-342.9169
AIC	691.8337
BIC	698.8259

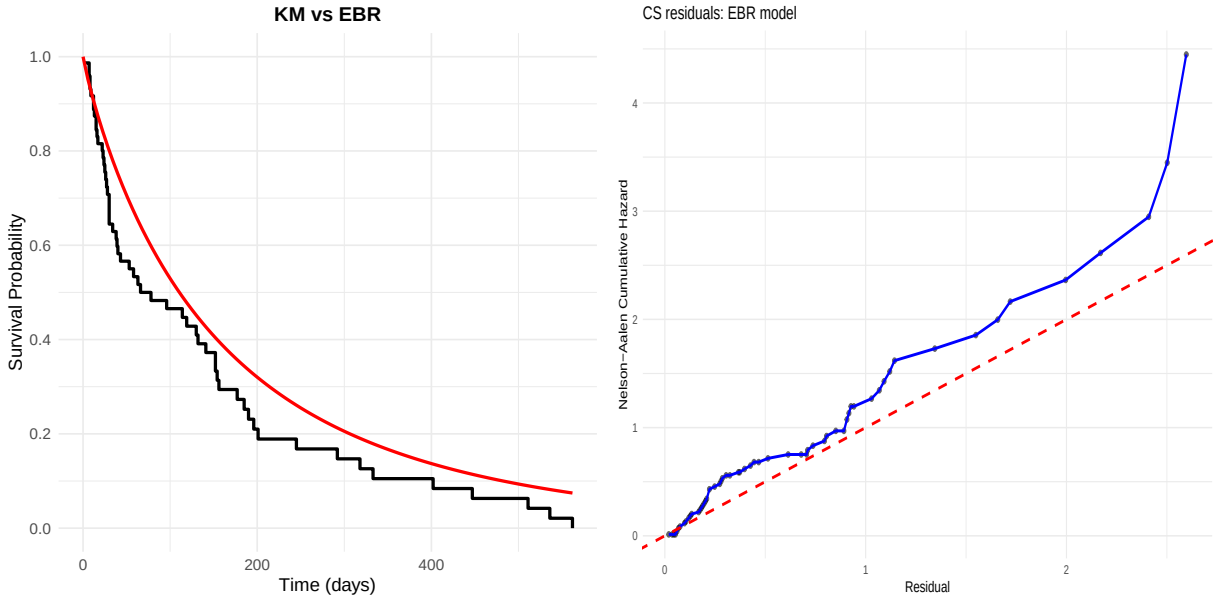

Figure 32. A graphic overview of the fitted EBR distribution and CS residual based on the BE.

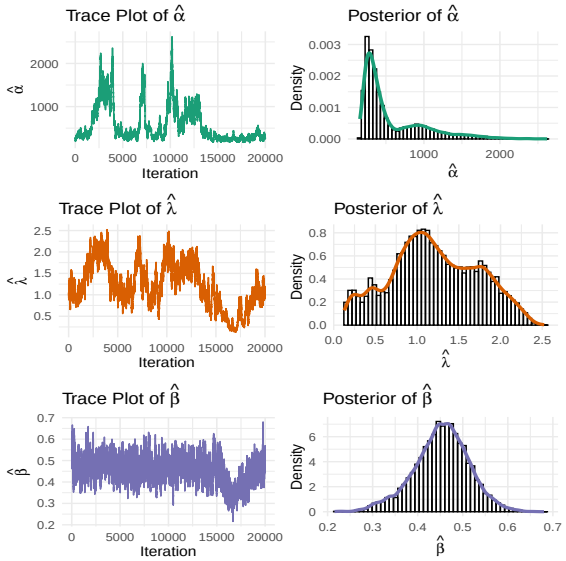

Figure 33. Trace plots and posterior PDFs of the estimated parameters ($\hat{\alpha}$, $\hat{\lambda}$ and $\hat{\beta}$).

8. Conclusions

In this study, we present a three-parameter EBR distribution in connection with the genesis of a truncated discrete Bell distribution. The proposed EBR distribution can handle heavy-tailed, overdispersed, and nonmonotonic hazard patterns that are frequent in many social and scientific studies. Key distributional characteristics, including the QF, RE, and ordinary moment, are derived to establish the theoretical foundation of the model. The prime focus of the study is to develop an economical (reducing time and cost) GASP for truncated life tests using the median as a quality index. Moreover, we employ both classical and Bayesian estimation methods to estimate parameters, executing sampling plans. We also compare the results with the plans proposed by [19, 22] using two real-life datasets. To investigate the validity of the estimates, we perform a simulation analysis, considering the bias, MSE, and CP of the estimates under both estimating techniques. We employ a censored data application to investigate the usefulness of the EBR distribution. The Kaplan–Meier survival curve supports the proposed EBR distribution. The overall conclusions of the analysis indicate that the EBR distribution stands apart based on the goodness-of-fit measures in comparison to other comparative distributions. Both estimation techniques work well; however, MLE is preferred for analysis of censored data. We believe the proposed distribution may be a suitable substitute for the traditional RD. The EBR distribution also demonstrates considerable potential for modeling censored survival data.

Author contributions

Laila A. Al-Essa: writing-review & editing, software, supervision, conceptualization and methodology and project administration; Muhammad Imran: validation, software, formal analysis and investigation; Farrukh Jamal: simulation, censored data analysis, and writing original draft. All authors have read and agreed to the published version of the manuscript.

Use of Generative-AI tools declaration

The authors declare they have not used Artificial Intelligence (AI) tools in the creation of this article.

Acknowledgments

Princess Nourah bint Abdulrahman University Researchers Supporting Project number (PNURSP2026R443), Princess Nourah bint Abdulrahman University, Riyadh, Saudi Arabia.

Conflict of interest

The authors declare no competing interests.

References

1. C. Ley, Flexible modelling in statistics: past, present and future, *J. Soc. Fr. Stat.*, **156** (2015), 76–96.
2. L. Rayleigh, On the resultant of a large number of vibrations of the same pitch and of arbitrary phase, *Philos. Mag.*, **10** (1880), 73–78.
3. D. Kundu, M. Z. Raqab, Generalized Rayleigh distribution: different methods of estimations, *Comput. Stat. Data Anal.*, **49** (2005), 187–200. https://doi.org/10.1016/j.csda.2004.05.008
4. G. M. Cordeiro, C. T. Cristino, E. M. Hashimoto, E. M. Ortega, The beta generalized Rayleigh distribution with applications to lifetime data, *Stat. Pap.*, **54** (2013), 133–161. https://doi.org/10.1007/s00362-011-0415-0
5. G. M. Cordeiro, G. M. Rodrigues, E. M. M. Ortega, L. H. de Santana, R. Vila, An extended Rayleigh model: properties, regression and COVID-19 application, *ArXiv*, 2022. https://doi.org/10.48550/arXiv.2204.05214
6. G. M. Cordeiro, M. Alizadeh, G. Ozel, B. Hosseini, E. M. M. Ortega, E. Altun, The generalized odd log-logistic family of distributions: properties, regression models and applications, *J. Stat. Comput. Simul.*, **87** (2017), 908–932. https://doi.org/10.1080/00949655.2016.1238088
7. A. A. Al-Babtain, A new extended Rayleigh distribution, *J. King Saud Univ. Sci.*, **32** (2020), 2576–2581. https://doi.org/10.1016/j.jksus.2020.04.015
8. F. Merovci, A three-parameter record-based transmuted Rayleigh distribution (order 3): theory and real-data applications, *Symmetry*, **17** (2025), 1034. https://doi.org/10.3390/sym17071034
9. M. Ganji, H. Bevrani, N. H. Golzar, S. Zabihi, The Weibull–Rayleigh distribution, some properties, and applications, *J. Math. Sci.*, **218** (2016), 269–277. https://doi.org/10.1007/s10958-016-3028-2
10. S. M. T. K. MirMostafaee, M. Mahdizadeh, A. J. Lemonte, The Marshall–Olkin extended generalized Rayleigh distribution: properties and applications, *Commun. Stat. Theory Methods*, **46** (2017), 653–671. https://doi.org/10.1080/03610926.2014.1002937
11. K. K. Jose, R. Sivadas, Negative binomial Marshall–Olkin Rayleigh distribution and its applications, *Econ. Qual. Control*, **30** (2015), 89–98. https://doi.org/10.1515/eqc-2015-0009

12. R. A. Bantan, C. Chesneau, F. Jamal, M. Elgarhy, M. H. Tahir, A. Ali, et al., Some new facts about the unit-Rayleigh distribution with applications, *Mathematics*, **8** (2020), 1954. https://doi.org/10.3390/math8111954
13. Y. M. Gómez, D. I. Gallardo, Y. Iriarte, H. Bolfarine, The Rayleigh–Lindley model: properties and applications, *J. Appl. Stat.*, **46** (2019), 141–163. https://doi.org/10.1080/02664763.2018.1458825
14. M. Aslam, C. H. Jun, A group acceptance sampling plan for truncated life test having Weibull distribution, *J. Appl. Stat.*, **36** (2009), 1021–1027. https://doi.org/10.1080/02664760802566788
15. A. Baklizi, A. E. Q. E. Masri, Acceptance sampling based on truncated life tests in the Birnbaum–Saunders model, *Risk Anal.*, **24** (2004), 1453–1457. https://doi.org/10.1111/j.0272-4332.2004.00541.x
16. M. Aslam, C. H. Jun, Y. L. Lio, M. Ahmad, M. Rasool, Group acceptance sampling plans for resubmitted lots under Burr-type XII distributions, *J. Chin. Inst. Ind. Eng.*, **28** (2011), 606–615. https://doi.org/10.1080/10170669.2011.651165
17. B. C. Nwankwo, H. O. Obiora-Ilouno, F. A. Almulhim, M. S. Mustafa, O. J. Obulezi, Group acceptance sampling plans for type-I heavy-tailed exponential distribution based on truncated life tests, *AIP Adv.*, **14** (2024), 035310. https://doi.org/10.1063/5.0194258
18. W. Hafeez, J. Du, N. Aziz, K. Ullah, W. K. Wong, M. Imran, et al., A Bayesian approach with double group sampling plan to estimate quality regions for proportion of nonconforming products in industry based on beta prior, *Commun. Stat. Simul. Comput.*, **54** (2025), 4442–4456. https://doi.org/10.1080/03610918.2024.2383650
19. A. Fayomi, K. Khan, A group acceptance sampling plan for another generalized transmuted-exponential distribution based on truncated lifetimes, *Qual. Reliab. Eng. Int.*, **40** (2024), 145–153. https://doi.org/10.1002/qre.3246
20. M. Imran, H. S. Bakouch, M. H. Tahir, M. Ameeq, F. Jamal, J. T. Mendy, A new Bell-exponential model: properties and applications, *Cogent Eng.*, **10** (2023), 2281062. https://doi.org/10.1080/23311916.2023.2281062
21. A. Algarni, Group acceptance sampling plan based on new compounded three-parameter Weibull model, *Axioms*, **11** (2022), 438. https://doi.org/10.3390/axioms11090438
22. A. M. Almarashi, K. Khan, C. Chesneau, F. Jamal, Group acceptance sampling plan using Marshall–Olkin Kumaraswamy exponential (MOKw-E) distribution, *Processes*, **9** (2021), 1066. https://doi.org/10.3390/pr9061066
23. H. M. Okasha, A. H. El-Baz, A. M. Basheer, Bayesian estimation of Marshall–Olkin extended inverse Weibull distribution using MCMC approach, *J. Indian Soc. Probab. Stat.*, **21** (2020), 247–257. https://doi.org/10.1007/s41096-020-00082-y
24. A. Z. Afify, S. Ahmed, M. Nassar, A new inverse Weibull distribution: properties, classical and Bayesian estimation with applications, *Kuwait J. Sci.*, **48** (2021), 3. https://doi.org/10.48129/kjs.v48i3.9896
25. M. Aslam, M. Azam, S. Balamurali, C. H. Jun, An economic design of a group sampling plan for a Weibull distribution using a Bayesian approach, *J. Test. Eval.*, **43** (2015), 1497–1503. https://doi.org/10.1520/JTE20140041
26. M. El-Morshedy, M. S. Eliwa, A. El-Gohary, E. M. Almetwally, R. El-Desokey, Exponentiated generalized inverse flexible Weibull distribution: Bayesian and non-Bayesian estimation under complete and type-II censored samples with applications, *Commun. Math. Stat.*, **10** (2022), 413–434. https://doi.org/10.1007/s40304-020-00225-4

27. E. A. Eldessouky, O. H. M. Hassan, M. Elgarhy, E. A. Hassan, I. Elbatal, E. M. Almetwally, A new extension of the Kumaraswamy exponential model with modeling of food chain data, *Axioms*, **12** (2023), 379. https://doi.org/10.3390/axioms12040379
28. N. Alsadat, M. Imran, M. H. Tahir, F. Jamal, H. Ahmad, M. Elgarhy, Compounded Bell-G class of statistical models with applications to COVID-19 and actuarial data, *Open Phys.*, **21** (2023), 20220242. https://doi.org/10.1515/phys-2022-0242
29. F. Castellares, S. L. Ferrari, A. J. Lemonte, On the Bell distribution and its associated regression model for count data, *Appl. Math. Model.*, **56** (2018), 172–185. https://doi.org/10.1016/j.apm.2017.12.014
30. Z. He, S. Wang, J. Shi, D. Liu, X. Duan, Y. Shang, Physics-informed neural network supported Wiener process for degradation modeling and reliability prediction, *Reliab. Eng. Syst. Saf.*, **258** (2025), 110906. https://doi.org/10.1016/j.ress.2025.110906
31. Z. He, S. Wang, D. Liu, A nonparametric degradation modeling method based on generalized stochastic process with B-spline function and Kolmogorov hypothesis test considering distribution uncertainty, *Comput. Ind. Eng.*, **203** (2025), 111036. https://doi.org/10.1016/j.cie.2025.111036
32. Z. He, S. Wang, D. Liu, A degradation modeling method based on artificial neural network supported Tweedie exponential dispersion process, *Adv. Eng. Inf.*, **65** (2025), 103376. https://doi.org/10.1016/j.aei.2025.103376
33. S. K. Maurya, S. Nadarajah, Poisson generated family of distributions: a review, *Sankhya B*, **83** (2021), 484–540. https://doi.org/10.1007/s13571-020-00237-8
34. M. H. Tahir, G. M. Cordeiro, Compounding of distributions: a survey and new generalized classes, *J. Stat. Distrib. Appl.*, **3** (2016), 13. https://doi.org/10.1186/s40488-016-0052-1
35. M. Shaked, J. G. Shantikumar, *Stochastic orders and their applications*, Springer, 1994. https://doi.org/10.1007/978-0-387-34675-5
36. S. Khan, O. S. Balogun, M. H. Tahir, W. Almutiry, A. A. Alahmadi, An alternate generalized odd generalized exponential family with applications to premium data, *Symmetry*, **13** (2021), 2064. https://doi.org/10.3390/sym13112064
37. M. Muhammad, B. Abba, J. Xiao, N. Alsadat, F. Jamal, M. Elgarhy, A new three-parameter flexible unit distribution and its quantile regression model, *IEEE Access*, **12** (2024), 156235–156251. https://doi.org/10.1109/ACCESS.2024.3485219
38. W. K. Hastings, Monte Carlo sampling methods using Markov chains and their applications, *Biometrika*, **57** (1970), 97–109. https://doi.org/10.1093/biomet/57.1.97
39. A. E. Gelfand, A. F. M. Smith, Sampling-based approaches to calculating marginal densities, *J. Amer. Stat. Assoc.*, **85** (1990), 398–409. https://doi.org/10.1080/01621459.1990.10476213
40. J. K. Kruschke, *Doing Bayesian data analysis: a tutorial with R, JAGS, and Stan*, Academic Press, 2014.
41. M. E. Ghitany, E. K. Al-Hussaini, R. A. Al-Jarallah, Marshall–Olkin extended Weibull distribution and its application to censored data, *J. Appl. Stat.*, **32** (2005), 1025–1034. https://doi.org/10.1080/02664760500165008
42. P. S. Sundaram, R. K. Radha, P. Venkatesan, Bayesian estimation of Weibull-G-Weibull distribution for censored data using M-H algorithm, *Adv. Appl. Stat.*, **91** (2024), 1095–1112. https://doi.org/10.17654/0972361724058

43. T. M. Therneau, P. M. Grambsch, *Modeling survival data: extending the Cox model*, Springer, 2000. https://doi.org/10.1007/978-1-4757-3294-8

Appendix

Appendix A

Table A.1. A numerical overview of μ, σ^2, γ_1, and γ_2 at some parametric values.

$\alpha = 1.5, \lambda = 2$					$\alpha = 1, \lambda = 0.15$				
β	μ	σ^2	γ_1	γ_2	β	μ	σ^2	γ_1	γ_2
0.50	0.1721	0.049	4.3617	40.421	0.50	0.8328	0.4169	1.0214	3.8670
0.55	0.2084	0.0574	3.7947	31.974	0.55	0.8817	0.4211	0.9634	3.7487
0.60	0.2458	0.0657	3.3577	26.158	0.60	0.9270	0.4236	0.9143	3.6576
0.65	0.2839	0.0737	3.0126	22.009	0.65	0.9693	0.4249	0.8723	3.5866
0.70	0.3223	0.0814	2.7342	18.957	0.70	1.0088	0.4251	0.8362	3.5307
0.76	0.3606	0.0887	2.5055	16.653	0.76	1.0458	0.4245	0.8048	3.4864
0.81	0.3987	0.0955	2.3147	14.873	0.81	1.0807	0.4234	0.7774	3.4511
0.86	0.4364	0.1018	2.1533	13.471	0.86	1.1135	0.4218	0.7533	3.4229
0.91	0.4735	0.1077	2.0152	12.348	0.91	1.1446	0.4199	0.7321	3.4002
0.96	0.5101	0.1132	1.8957	11.434	0.96	1.1741	0.4177	0.7133	3.3820
1.01	0.5459	0.1181	1.7915	10.681	1.01	1.2020	0.4153	0.6965	3.3675
1.06	0.581	0.1227	1.6998	10.054	1.06	1.2286	0.4128	0.6816	3.3559
1.11	0.6153	0.1269	1.6186	9.5254	1.11	1.2540	0.4102	0.6682	3.3466
1.16	0.6489	0.1306	1.5462	9.0762	1.16	1.2782	0.4075	0.6562	3.3394
1.21	0.6817	0.1341	1.4813	8.6913	1.21	1.3014	0.4048	0.6454	3.3338
1.27	0.7137	0.1372	1.4228	8.3590	1.27	1.3236	0.4020	0.6357	3.3295
1.32	0.7449	0.1400	1.3699	8.0702	1.32	1.3449	0.3992	0.6269	3.3264
1.37	0.7754	0.1426	1.3219	7.8177	1.37	1.3653	0.3965	0.6189	3.3242
1.42	0.8051	0.1449	1.2780	7.5957	1.42	1.3850	0.3937	0.6117	3.3228
1.47	0.8341	0.1469	1.2379	7.3995	1.47	1.4040	0.3910	0.6052	3.3221
1.52	0.8624	0.1488	1.2010	7.2253	1.52	1.4222	0.3883	0.5992	3.3220
1.57	0.8900	0.1504	1.1671	7.0701	1.57	1.4398	0.3857	0.5938	3.3223
1.62	0.9170	0.1519	1.1358	6.9311	1.62	1.4569	0.3830	0.5889	3.3230
1.67	0.9433	0.1532	1.1068	6.8062	1.67	1.4733	0.3805	0.5844	3.3241
1.72	0.9689	0.1544	1.0799	6.6937	1.72	1.4892	0.3779	0.5803	3.3254
1.78	0.9940	0.1555	1.0549	6.5919	1.78	1.5046	0.3754	0.5765	3.3270
1.83	1.0185	0.1564	1.0316	6.4996	1.83	1.5196	0.3730	0.5731	3.3288
1.88	1.0424	0.1572	1.0099	6.4157	1.88	1.5341	0.3706	0.5700	3.3308
1.93	1.0657	0.1579	0.9896	6.3392	1.93	1.5482	0.3683	0.5671	3.3329
1.98	1.0886	0.1584	0.9706	6.2693	1.98	1.5619	0.3660	0.5645	3.3352
2.03	1.1109	0.1590	0.9527	6.2052	2.03	1.5751	0.3637	0.5622	3.3375
2.08	1.1327	0.1594	0.9360	6.1464	2.08	1.5881	0.3615	0.5600	3.3399
2.13	1.1540	0.1598	0.9202	6.0923	2.13	1.6007	0.3593	0.5580	3.3424
2.18	1.1749	0.1600	0.9054	6.0425	2.18	1.6129	0.3572	0.5563	3.3450
2.23	1.1954	0.1603	0.8914	5.9965	2.23	1.6249	0.3551	0.5546	3.3476
2.29	1.2154	0.1605	0.8782	5.9540	2.29	1.6365	0.3531	0.5531	3.3502
2.34	1.2350	0.1606	0.8657	5.9146	2.34	1.6479	0.3511	0.5518	3.3529
2.39	1.2542	0.1607	0.8539	5.8781	2.39	1.6590	0.3492	0.5506	3.3556
2.44	1.2730	0.1607	0.8427	5.8442	2.44	1.6698	0.3473	0.5495	3.3583
2.49	1.2915	0.1607	0.8321	5.8126	2.49	1.6804	0.3454	0.5485	3.3610
2.54	1.3096	0.1606	0.8221	5.7833	2.54	1.6907	0.3436	0.5476	3.3638
2.59	1.3273	0.1606	0.8125	5.7559	2.59	1.7008	0.3418	0.5468	3.3665
2.64	1.3447	0.1605	0.8035	5.7303	2.64	1.7107	0.3400	0.5461	3.3692
2.69	1.3617	0.1603	0.7948	5.7065	2.69	1.7204	0.3383	0.5455	3.3719
2.74	1.3785	0.1602	0.7866	5.6841	2.74	1.7299	0.3366	0.5449	3.3746
2.80	1.3949	0.1600	0.7788	5.6632	2.80	1.7392	0.3349	0.5444	3.3773
2.85	1.4111	0.1598	0.7713	5.6437	2.85	1.7483	0.3333	0.5440	3.3800
2.90	1.4269	0.1596	0.7642	5.6253	2.90	1.7572	0.3317	0.5436	3.3827
2.95	1.4425	0.1594	0.7574	5.6081	2.95	1.7659	0.3301	0.5433	3.3854
3.00	1.4578	0.1591	0.7509	5.5919	3.00	1.7745	0.3286	0.5431	3.3880

Table A.2. A numerical overview of RE of the EBR distribution at some parametric values.

$\lambda = 0.3, \lambda = 2, \lambda = 4$					$\lambda = 0.3, \lambda = 2, \lambda = 4$				
β	a	RE	RE	RE	β	a	RE	RE	RE
0.50	0.50	0.935	-0.573	-3.615	3.00	3.00	0.581	-0.205	-0.948
1.00	0.50	1.055	0.082	-1.566	3.50	3.00	0.558	-0.214	-0.923
1.50	0.50	1.063	0.255	-0.977	4.00	3.00	0.538	-0.225	-0.911
2.00	0.50	1.050	0.314	-0.733	4.50	3.00	0.520	-0.237	-0.907
2.50	0.50	1.032	0.333	-0.613	5.00	3.00	0.503	-0.249	-0.907
3.00	0.50	1.014	0.336	-0.550	0.50	3.50	0.404	-1.809	-4.533
3.50	0.50	0.997	0.332	-0.515	1.00	3.50	0.657	-0.518	-1.951
4.00	0.50	0.981	0.324	-0.495	1.50	3.50	0.643	-0.302	-1.349
4.50	0.50	0.967	0.314	-0.485	2.00	3.50	0.612	-0.244	-1.123
5.00	0.50	0.954	0.304	-0.481	2.50	3.50	0.583	-0.230	-1.022
0.50	1.50	0.603	-1.439	-4.217	3.00	3.50	0.556	-0.232	-0.972
1.00	1.50	0.800	-0.346	-1.815	3.50	3.50	0.533	-0.240	-0.947
1.50	1.50	0.794	-0.133	-1.211	4.00	3.50	0.512	-0.252	-0.935
2.00	1.50	0.768	-0.072	-0.979	4.50	3.50	0.494	-0.264	-0.931
2.50	1.50	0.742	-0.056	-0.872	5.00	3.50	0.478	-0.276	-0.932
3.00	1.50	0.718	-0.056	-0.819	0.50	4.00	0.378	-1.853	-4.573
3.50	1.50	0.696	-0.063	-0.792	1.00	4.00	0.639	-0.539	-1.969
4.00	1.50	0.677	-0.074	-0.778	1.50	4.00	0.623	-0.322	-1.366
4.50	1.50	0.659	-0.085	-0.773	2.00	4.00	0.592	-0.265	-1.142
5.00	1.50	0.644	-0.097	-0.772	2.50	4.00	0.562	-0.251	-1.041
0.50	2.00	0.530	-1.585	-4.337	3.00	4.00	0.536	-0.253	-0.991
1.00	2.00	0.746	-0.414	-1.866	3.50	4.00	0.513	-0.262	-0.967
1.50	2.00	0.737	-0.199	-1.262	4.00	4.00	0.492	-0.273	-0.955
2.00	2.00	0.709	-0.139	-1.033	4.50	4.00	0.474	-0.285	-0.951
2.50	2.00	0.681	-0.123	-0.929	5.00	4.00	0.457	-0.298	-0.952
3.00	2.00	0.656	-0.125	-0.877	0.50	4.50	0.355	-1.889	-4.606
3.50	2.00	0.634	-0.132	-0.850	1.00	4.50	0.623	-0.556	-1.983
4.00	2.00	0.614	-0.143	-0.838	1.50	4.50	0.607	-0.339	-1.381
4.50	2.00	0.596	-0.155	-0.833	2.00	4.50	0.576	-0.282	-1.157
5.00	2.00	0.580	-0.167	-0.833	2.50	4.50	0.546	-0.268	-1.057
0.50	2.50	0.477	-1.683	-4.422	3.00	4.50	0.519	-0.271	-1.007
1.00	2.50	0.708	-0.459	-1.902	3.50	4.50	0.496	-0.279	-0.983
1.50	2.50	0.697	-0.243	-1.299	4.00	4.50	0.475	-0.291	-0.971
2.00	2.50	0.668	-0.184	-1.071	4.50	4.50	0.456	-0.303	-0.968
2.50	2.50	0.639	-0.169	-0.968	5.00	4.50	0.440	-0.316	-0.968
3.00	2.50	0.613	-0.171	-0.917	0.50	5.00	0.336	-1.920	-4.634
3.50	2.50	0.591	-0.179	-0.892	1.00	5.00	0.610	-0.570	-1.996
4.00	2.50	0.571	-0.190	-0.880	1.50	5.00	0.594	-0.354	-1.394
4.50	2.50	0.553	-0.202	-0.875	2.00	5.00	0.562	-0.296	-1.170
5.00	2.50	0.536	-0.214	-0.875	2.50	5.00	0.532	-0.283	-1.070
0.50	3.00	0.436	-1.754	-4.484	3.00	5.00	0.505	-0.285	-1.021
1.00	3.00	0.680	-0.493	-1.930	3.50	5.00	0.481	-0.294	-0.997
1.50	3.00	0.666	-0.276	-1.327	4.00	5.00	0.461	-0.306	-0.985
2.00	3.00	0.636	-0.218	-1.100	4.50	5.00	0.442	-0.318	-0.982
2.50	3.00	0.607	-0.203	-0.998	5.00	5.00	0.425	-0.331	-0.982

Appendix B

R codes for estimation

```
# Required packages

install.packages("AdequacyModel")
install.packages("VGAM")
library(AdequacyModel)
library(VGAM)
```

```
# Data

x <- c(
  1.12,0.17,0.64,4.32,1.22,0.37,1.16,1.42,0.09,1.67,
  0.13,0.25,0.08,0.04,2.35,0.20,0.78,0.34,1.02,0.17,
  1.76,2.39,0.50,1.35,3.36,0.45,0.90,2.92,6.53,1.62,
  7.46,3.19,2.49,1.40,7.49,0.57,0.14,0.63,5.23,0.71,
  0.68,0.12,0.09,3.47,5.93,1.82,4.20,7.29,3.13,3.41)
# PDF of EBR model

pdf_EBellR <- function(par, x) {
  alpha  <- par[1]
  beta   <- par[2]
  lambda <- par[3]

  G <- prayleigh(x, alpha)
  g <- drayleigh(x, alpha)

  num <- beta * lambda * g *
    Gˆ(beta - 1) *
    exp(lambda * (1 - Gˆbeta)) *
    exp(-exp(lambda) * (1 - exp(-lambda * Gˆbeta)))

  den <- (1 - exp(1 - exp(lambda)))

  return(num / den)}

# CDF of EBR model

cdf_EBellR <- function(par, x) {
  alpha  <- par[1]
  beta   <- par[2]
  lambda <- par[3]

  G <- prayleigh(x, alpha)

  F <- (1 - exp(-exp(lambda) * (1 - exp(-lambda * Gˆbeta)))) /
       (1 - exp(1 - exp(lambda)))

  return(F)
}

# Goodness-of-fit
```

```
res_EBR <- goodness.fit(
  pdf    = pdf_EBellR,
  cdf    = cdf_EBellR,
  starts = c(1.4, 0.07, 2.31),
  data   = x,
  method = "B",
  domain = c(0, Inf),
  mle    = NULL)
res_EBR
```

```
# Bayesian Estimation
# Required packages
install.packages("HDInterval")
library(HDInterval)
# Data

datta <- c(1.12,0.17,0.64,4.32,1.22,0.37,1.16,1.42,0.09,1.67,
           0.13,0.25,0.08,0.04,2.35,0.20,0.78,0.34,1.02,0.17,
           1.76,2.39,0.50,1.35,3.36,0.45,0.90,2.92,6.53,1.62,
           7.46,3.19,2.49,1.40,7.49,0.57,0.14,0.63,5.23,0.71,
           0.68,0.12,0.09,3.47,5.93,1.82,4.20,7.29,3.13,3.41)
x <- sort(datta)

# MCMC setup

N <- 10000
alpha  <- lambda <- beta <- numeric(N)
alpha[1]  <- 0.1
lambda[1] <- 0.1
beta[1]   <- 0.1

# log-likelihood function

loglik <- function(alpha, beta, lambda, x){

  G <- prayleigh(x, alpha)
  g <- drayleigh(x, alpha)

  f <- beta * lambda * g *
    Gˆ(beta - 1) *
    exp(lambda * (1 - Gˆbeta)) *
    exp(-exp(lambda) * (1 - exp(-lambda * Gˆbeta))) /
    (1 - exp(1 - exp(lambda)))
```

```
  sum(log(f))}
# MCMC loop
for(i in 2:N){

  # -------- alpha --------
  repeat{
    alpha11 <- alpha[i-1] + rnorm(1,0,0.5)
    if(alpha11 > 0) break
 }

  La  <- loglik(alpha[i-1], beta[i-1], lambda[i-1], x)
  La1 <- loglik(alpha11,   beta[i-1], lambda[i-1], x)

  Pa  <- dgamma(alpha[i-1], 8, 5, log=TRUE)
  Pa1 <- dgamma(alpha11,   8, 5, log=TRUE)

  ra <- (La1 - La) + (Pa1 - Pa)

  if(!is.na(ra) && log(runif(1)) < ra){
    alpha[i] <- alpha11
  } else {
    alpha[i] <- alpha[i-1]
  }

  # -------- lambda --------
  repeat{
    lambda11 <- lambda[i-1] + rnorm(1,0,0.5)
    if(lambda11 > 0) break
  }

  Ll  <- loglik(alpha[i], beta[i-1], lambda[i-1], x)
  Ll1 <- loglik(alpha[i], beta[i-1], lambda11,   x)

  Pl  <- dgamma(lambda[i-1], 2, 0.9, log=TRUE)
  Pl1 <- dgamma(lambda11,   2, 0.9, log=TRUE)

  rl <- (Ll1 - Ll) + (Pl1 - Pl)

  if(!is.na(rl) && log(runif(1)) < rl){
    lambda[i] <- lambda11
  } else {
    lambda[i] <- lambda[i-1]
  }
```

```
  # -------- beta --------
  repeat{
    beta11 <- beta[i-1] + rnorm(1,0,0.5)
    if(beta11 > 0) break
  }

  Lb  <- loglik(alpha[i], beta[i-1], lambda[i], x)
  Lb1 <- loglik(alpha[i], beta11,    lambda[i], x)

  Pb  <- dgamma(beta[i-1], 12, 4.5, log=TRUE)
  Pb1 <- dgamma(beta11,   12, 4.5, log=TRUE)

  rb <- (Lb1 - Lb) + (Pb1 - Pb)

  if(!is.na(rb) && log(runif(1)) < rb){
    beta[i] <- beta11
  } else {
    beta[i] <- beta[i-1]
  }
}

# Burn-in (80%)
burn <- floor(0.2 * N)
c1 <- alpha[(burn+1):N]
c2 <- beta[(burn+1):N]
c3 <- lambda[(burn+1):N]

# HPD intervals

hpda <- HDInterval::hdi(c1, credMass=0.95)
hpdb <- HDInterval::hdi(c2, credMass=0.95)
hpdl <- HDInterval::hdi(c3, credMass=0.95)

# Bayesian estimates
BESEL <- c(mean(c1), mean(c2), mean(c3))
HPD_alpha <- c(hpda[1], hpda[2])
HPD_beta  <- c(hpdb[1], hpdb[2])
HPD_lambda<- c(hpdl[1], hpdl[2])
```